Chapter 4

Terrestrial radiation

Gamma radiation from terrestrial sources is an important component of the natural radiation environment. Natural sources of terrestrial gamma radiation are considered in the light of mapping the dose rate from gamma rays emitted by these sources. In this respect, the radioactivity properties of potassium (K), thorium (Th) and uranium (U) are of particular interest, because terrestrial gamma radiation is mostly caused by isotopes of the radioactive decay series of ^{238}U, ^{232}Th, ^{235}U and the radioactive isotope ^{40}K. With a half-life of 1 248 million years, ^{40}K is a long-lived isotope and represents 0.0117 % of the total mass of potassium. Since the presence of ^{235}U in natural uranium is only 0.72 %, a more significant source of gamma radiation is the ^{238}U decay series. In both the ^{238}U and ^{232}Th series, gamma radiation is mainly emitted by their daughter products, and not by the parent isotopes.

The radioactivity levels of rocks can vary considerably depending on their type. The presence of radioactive elements in soils is mostly governed by the parent rock and the climatic conditions in the region. Due to their interaction with matter, gamma rays rarely penetrate more than tens of centimetres in soil/rocks. Actually, about 95 % of terrestrial gamma radiation above the Earth's surface originates from the top 35 cm surface layer of the rock-soil medium.

This chapter discusses methods for mapping terrestrial dose rate, which is only component of gamma dose rate in the environment, as well as decomposition of signals from gamma detectors. Also addressed are the spatial and temporal variability of natural terrestrial dose rate and the variability of dose rate from nuclear fallout.

Terrestrial gamma dose rate can be determined by measurements or indirectly by using geochemical data. Experimentally, the dose rate can be determined either by total count rate measurements or by field gamma-ray spectrometry. In both cases, calibrating radiometric instruments is fundamental for correctly converting measurement data into dose rate. Opportunities for using measurement data generated by European countries and transferred to the European Radiological Data Exchange Platform (EURDEP) System are discussed. Prospects for using new types of spectrometric detectors and new monitoring techniques are outlined.

Within the indirect approach, TGDR is determined by using activity concentrations of ^{40}K, ^{238}U and ^{232}Th, respectively, in rock-soil medium (according to UNSCEAR, 2008). This approach has been used to create the European Terrestrial Gamma Dose Rate Map (in nGy/h). Furthermore, TGDR is converted to external effective dose to adults. The European Annual Terrestrial Gamma Dose Map shows the annual effective dose (in mSv) that a person would receive from terrestrial radiation, if she/he spends all the reference time in a location where the soil has fixed U, Th and K concentrations.

Clockwise from top-left:

Outcrops of dunite, serpentinised peridotite and clinopyroxene-rich coarse gabbro around Bonassola (Liguria, Italy). They are rocks with low activity concentrations of natural radionuclides.
Source: Giorgia Cinelli.

Pyroclastic deposit in the Vulsini Volcanic District, an area characterised by a high natural background radiation (Latium, Italy).
Source: Giorgia Cinelli.

A crop field in the Vulsini Volcanic District, an area characterised by a high natural background radiation (Latium, Italy).
Source: Giorgia Cinelli.

In situ gamma spectrometry measurement in the Vulsini Volcanic District, an area characterised by a high natural background radiation (Latium, Italy).
Source: Giorgia Cinelli.

View of Pitigliano, a town built on tuff with volcanic rocks (Latium, Italy).
Source: Laura Tositti.

Terrestrial radiation

This chapter discusses natural sources of terrestrial radiation, their radiological properties as gamma radiation, and the relevance of mapping dose rate generated by gamma rays which are emitted by these sources. Moreover, the European Terrestrial Gamma Dose Rate Map is shown.

4.1 Source of terrestrial natural radiation

Terrestrial radiation, a significant component of the natural radiation environment, is generated by natural radionuclides in rocks and reflects the Earth's surface geological setting. More than twenty primordial natural radionuclides in rocks, formed during the origin of the Earth 4.6 billion years ago, are the sources of alpha, beta and gamma radiation in rocks. Due to their contents in rocks and their radiation intensity, primordial radionuclides of potassium (K), thorium (Th) and uranium (U) are the fundamental sources of radioactivity in rocks. The half-lives of prominent natural radionuclides are very long (e.g. for ^{40}K, $T_{1/2}$ = 1.3 * 10^9 a; for ^{238}U, $T_{1/2}$ = 4.47 * 10^9; and for ^{232}Th, $T_{1/2}$ = 1.39 * 1 0^{10} a), and K, U and Th are permanent sources of terrestrial radiation (more details in Section 2.2 and Chapter 3). Uranium and thorium form natural decay series whose decay products contribute to overall terrestrial radiation. Radioactivity of rocks is predominantly determined by the detection of gamma rays and expressed as gamma dose rate (Gy/s, practically nGy/h), or as the contents of single radionuclides. The gamma dose rates generated individually by K, Th or U in rocks of the Earth's crust are of the same order of magnitude.

Among primordial gamma-radiating radionuclides which have no radiological importance in our context, are ^{50}V, ^{87}Rb, ^{138}La and ^{176}Lu (more details in Section 2.2).

4.1.1 Radioactivity properties of K, Th and U

Potassium (K) is an alkali metal (with one main oxidation state: +1) with an atomic mass of 39 and three natural isotopes, including two stable ones, ^{39}K (93.2581 % of K total mass), ^{41}K (6.7302 % of K total mass), and the long-lived (1248 million years half-life) radioactive ^{40}K (0.0117 %). The latter decays either to ^{40}Ca (89.28 %) by emitting a beta particle, or to gas ^{40}Ar (10.72 %) by emitting a gamma ray with energy of 1.46 MeV after electron capture (Figure 4-1a).

Figure 4-1 presents gamma-ray energy emission line spectra of potassium, uranium decay series and thorium decay series. Simplified gamma-ray spectra illustrate the most significant energy lines contributing to terrestrial gamma dose rate and are used for radioelement analyses. Since ^{40}K occurs as a fixed proportion of K, these gamma rays can be used to estimate the total amount of K present in analysed rocks. The determination of K by gamma-ray spectrometry is direct. The relationship between units of mass concentration of potassium and its specific activity is 10 g/kg K ~ 313 Bq/kg of ^{40}K (IAEA, 1989). By emitting ~ 3.1 gamma quanta/s per 1 g K, potassium contributes to terrestrial gamma dose rate.

Potassium is a widespread element in the lithosphere, with the highest concentrations occurring in magmatic and metamorphic rocks containing potassium: namely, feldspars, leucite, nepheline, biotite, muscovite, sericite and phlogopite. An increased concentration of potassium is common in pegmatites and clays and accompanies alterations at some deposits. Potassium is mobile in the geological environment. Potassium (K) is preserved in the Earth´s upper crust in concentrations between 20 and 25 g/kg K.

Thorium (Th) is an actinide-series element with an atomic number of 90 and an atomic mass of 232. Thorium is radioactive with one main natural isotope, the primordial, long-lived radionuclide ^{232}Th, which has the longest half-life (1.405 × 10^{10} years) of all known radioactive isotopes and comprises 99.98 % of the total mass of Th. Thorium decays through a long radioactive decay series, ending with the stable lead isotope ^{208}Pb.

Energy emitted by gamma rays of isotopes of ^{232}Th decay series is in the range up to 2.615 MeV (Figure 4-1b). Since ^{232}Th is not a source of gamma rays, analysis of thorium in rock environment is performed by detecting gamma rays of suitably selected daughter products in the ^{232}Th decay series (see Section 2.1). The relationship between mass concentration of thorium and its specific activity is given by 1 mg/kg Th ~ 4.06 Bq/kg of ^{232}Th (IAEA, 1989).

Thorium, with many complex geochemical forms, occurs in increased amounts in accessory minerals such as zircon, monazite, allanite, sphene, xenotime and apatite. Thorium in tetravalent state exhibits low solubility. Thorium (Th) crustal abundance is 7 – 12 mg/kg Th.

Uranium (U) is a heavy actinide-series element (with an atomic number of 92) with two main natural, primordial, long-lived radionuclides, including the more abundant ^{238}U (half-life of 4.5 × 10^9 years, 99.274 % of the total mass of U) and the less abundant ^{235}U (half-life of 7.0 × 10^8 years, 0.72 % of the total mass of U), both decaying separately through long and complex radioactive decay series, ending with stable lead isotopes (^{206}Pb and ^{207}Pb, respectively). Another natural uranium isotope ^{234}U (half-life of 2.4 × 10^5 years, 0.0056 % of total natural uranium), is the third decay product in the ^{238}U radioactive decay series. This uranium isotope is generally considered in equilibrium (to slightly deficient) with its progenitor ^{238}U. The ^{238}U/^{235}U ratio has increased over time due to faster radioactive decay of ^{235}U, being at present 137.5 ± 0.5 (Wedepohl, 1978a).

The ^{238}U and ^{235}U isotopes are mother elements of decay series, whose daughter elements are sources of alpha, beta and gamma radiation. The ^{238}U series is more important as a source of gamma radiation in rocks than is the ^{235}U series, since the presence of ^{235}U in natural uranium is low (0.72 %). The energy of emitted gamma rays of ^{238}U decay series is generally in the interval of 0 – 2.2 MeV, while single energy lines are typical for individual radionuclides (Figure 4-1c). Analysis of U in rocks is mostly carried out by detecting selected energy of gamma rays of daughter products of the ^{238}U decay series. Conversion between mass concentration of natural uranium and its ^{238}U specific activity is given by the relation: 1 mg/kg U ~ 12.35 Bq/kg of ^{238}U or ^{226}Ra (IAEA, 1989). Specific gamma-ray emission of U is approximately given as ~ 33 gamma quanta/s per 1 g U (Kogan et al., 1969).

Uranium in rocks has many complex geochemical forms and occurs in primary uranium minerals and secondary uranium minerals formed under oxydation. Minerals with uranium as a major constituent include uraninite (pitchblende), betafite, coffinite, while those with uranium as a minor constituent include zircon, xenotime, monazite, orthite, apatite and sphene. Uranium in tetravalent state is generally geochemically stable, while uranium in its hexavalent state is soluble and mobile in the geological environment, and as a result the radioactive equilibrium in ^{238}U decay series can be disturbed due to uranium mobility. Uranium has an average crustal abundance of 2 – 3 mg/kg U.

4.1.2 Radioactivity as a function of rock type (see also Chapter 3)

Natural radionuclide contents vary widely between and within different types of rock (magmatic, metamorphic, sedimentary). The radioctivity levels of magmatic rocks tend to increase with the acidity of the rocks. Granite, granodiorite and syenite are usually highly radioactive, while basic and ultrabasic magmatic rocks are characterised by extremely low radioactivity. The radioactivity of sedimentary rocks is mostly related to the composition of material undergoing sedimentation. Enhanced radioactivity has been observed in clays, phosphates, potassium salts and bituminous sediments. Limestones, gypsum and quartzites all belong to the least radioactive sediments. The radioactivity of the metamorphosed rocks corresponds mainly to the primary rock material. Some orthogneisses and composite gneisses (migmatites) display fairly high activity, whereas amphibolites and serpentinites belong to the least radioactive. Fluidal magma component penetrating crystalline rocks can be enriched by potassium or silicates which enhances or reduces rock radioactivity. The presence of radioactive elements in soil is mostly governed by the parent rock and climatic conditions of the region. Depending on the solubility of radioactive elements and the direction of water inflow or evaporation, the soil may either be enriched or depleted by single radionuclides. General trends show a 0 – 30 % relative decrease in radioactive elements in soils in comparison with the radioactive elements in the geological basement (Dickson & Scott, 1997; IAEA, 2003).

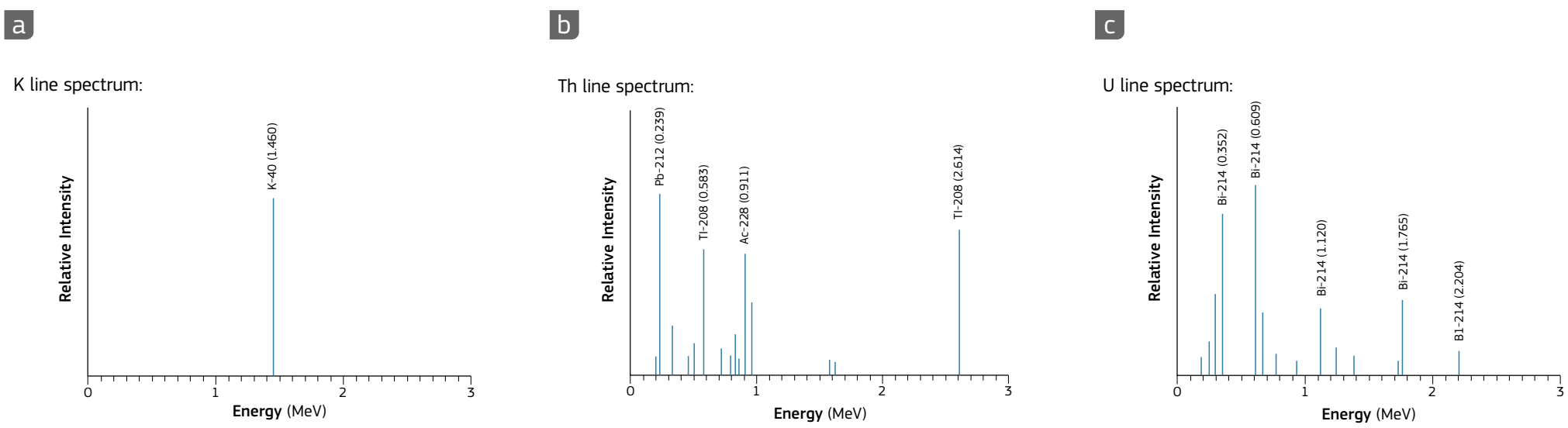

Figure 4-1.
Gamma-ray energy emission line spectra of potassium, thorium and uranium.
Source: IAEA, 2003.

Example: Variability of K, Th and U concentrations in the Czech Republic

While the radioactivity of identical lithological types of rocks in single European countries varies, the current contents of radioelements in some rocks are illustrative. For example, Table 4-1 introduces typical low and enhanced contents of K, Th and U in rocks of the Bohemian Massif, Czech Republic, and corresponding terrestrial gamma dose rate. Data in Table 4-1 do not correspond to the extremely high radioactivity values found in Cambrian Alum shales in Scandinavia or those of local volcanic rocks found in southern Europe. Numerous illustrative data on radioactivity of rocks, their contents of K, Th and U and their research have been published (Matolin, 2017).

Locality	Rock	K	Th	U	Dose rate
		g/kg	mg/kg	mg/kg	nGy/h
1 Adršpach	sandstone	1	2.1	0.6	9.9
2 Krucemburk	sandstone	9	4.2	1.8	33
3 Příbram	schist, graywacke	10	5.2	2.4	40
4 Dol. Rožínka	paragneiss	17	8.7	3.5	63.9
5 Říp	alkaline basalt	12	13.6	3.4	68.9
6 Příbram	granodiorite	20	13	3.4	78.5
7 Budišov	durbachite	32	24	5.9	135.2
8 Bezděz	phonolite	51	32	8.6	195.3
9 Teplice - Cínovec	rhyolite	47	41	12	231.6

Table 4-1.
Typical concentrations of K, Th and U in rocks of the Bohemian massif, Czech Republic, and the corresponding terrestrial gamma dose rate.
Source: Matolin, M., data of field gamma-ray spectrometry from various projects on radioactivity of rocks in the Czech Republic.

Figure 4-2.
Index map of the Czech Republic with localities quoted in the Table 4-1.
Source: Data on field gamma-ray spectrometry from various projects on radioactivity of rocks in the Czech Republic (Matolin, 2017); modified by Lovell Johns.

4.1.3 Terrestrial gamma rays in the environment

The gamma-ray field of a rock - soil medium (terrestrial radiation) is generated by the natural radionuclides in rocks - soils and is affected by the composition and physical state of rocks - soils. Gamma radiation is defined as electromagnetic radiation with wavelength on the order of 10^{-12}m and frequency on the order of 10^{18} Hz. Gamma rays emitted by natural radionuclides, in rocks primarily by K, Th and U, penetrate through matter. The photoelectric effect, Compton scattering and pair production are the fundamental processes by which gamma rays interact with atoms in matter. The cross section (probability of interaction) is a function of their energy and the elemental composition of the matter. The gamma rays are partly absorbed or their emission energy decreases gradually through Compton scattering.

The dispersion of gamma radiation above various geological sources depends on source radioelement, source physical dimensions, and on the detector – source geometry. Gamma radiation of a certain energy emitted by a point source (small geological surface object) is determined by the relation:

$$I_r = \frac{k * m}{r^2} e^{-\mu r} \qquad (4\text{-}1)$$

where:
k is the constant expressing gamma radiation of a particular radionuclide;
m (kg) is the mass of the radionuclide;
r (m) is the distance from source to detector; and
μ (m^{-1}) is the linear attenuation coefficient of gamma rays along their path.
The linear attenuation coefficient μ depends on the gamma energy and on the composition of the medium. The unscattered gamma-ray field of an infinite plane geological body at height h is attenuated at height h according to the relation:

$$I_h = I_0 * E_2(\mu h) \qquad (4\text{-}2)$$

where:
I_0 is the ground intensity of radiation; and
$E_2(\mu h)$ is the integral exponential function of the second kind for the argument μh.

While attenuation of gamma rays with distance r from a point source is significant, the gamma-ray field over an infinite rock source (the Earth's surface) at an altitude of h = 80 m is approximately one half of the ground value I_0.

Physical models of gamma-ray fields define sources of gamma radiation, its geometry, intensity and energy of gamma rays, elemental composition and geometry of absorbing media, distance between the source and point of gamma-ray field evaluation, and attenuation of gamma rays in the matter. Literature (e.g. Mares et al., 1984; Grasty, 1987; IAEA, 1989; ICRU, 1994; IAEA, 2003) introduces various mathematical models enabling estimates of gamma-ray fields of point sources, linear sources and three-dimensional sources of gamma radiation, the latter modelling geological environment. Specification of gamma-ray detectors is fundamental for estimating radiometric measurements and their precision and errors (more details about detectors in Section 2.5). Attenuation of gamma rays in the rock environment limits their penetration range. Theory and experiments show that gamma rays generated by natural radionuclides in rocks are nearly absorbed by any media having the area density 100 g/cm^2. Thus 95 % of the gamma radiation recorded on the Earth's surface originates from the top 35 cm of the soil.

Various environmental effects change the gamma-ray field over rocks. The significant parameters are soil moisture, surface snow layer, mass of surface vegetation, precipitation of air radon (^{222}Rn) daughter products (^{214}Pb and ^{214}Bi) which leads to an instant increase of surface gamma radiation, changes of radon emanation power, temperature and pressure effects on the atmospheric air density and its gamma rays attenuation, and topography and its geometrical effects.

Terrestrial gamma dose rate (see below for definition) is just one component registered on the Earth's surface. A gamma radiometric instrument on the surface registers terrestrial radiation, cosmic radiation, gamma rays of daughter products of aerial radon, internal radioactivity of radiometric equipment and the platform and nuclear fallout (see Section 4.2.4). In geophysical rock radiometric mapping, radiation originating not from the rock environment is regarded as 'background'; i.e. caesium-137 (^{137}Cs) contamination is removed during data processing.

4.2 Dose rate

4.2.1 Ambient dose rate

Ambient dose rate (ADR) is the generic term used for dose rate at a location, usually in free air.

a. Kerma and absorbed dose

The kerma ('kinetic energy released per unit mass' (acronym: kerma)), denoted K, is the total initial kinetic energy of all charged particles set free by uncharged particles (photons, neutrons) per unit mass of a medium. It is expressed in units of gray (Gy), 1 Gy = 1 J/kg. The energy which is actually deposited in and therefore absorbed by or imparted to the mass element, is called absorbed dose (D) in a medium, again expressed in Gy. The difference between kerma and absorbed dose lies in the fact that part of the energy set free in the mass (i.e. kerma) escapes and is deposited outside. Therefore K ≥ D. This effect is important for higher incident energy. For example, bremsstrahlung escapes and is not deposited in the mass element, but outside, and is not counted as absorbed dose. For exact definitions, see ICRU (2011). Environmental dose rates are frequently reported as kerma rates in nGy/h. While lower gamma energies are typical of most ambient radiation, kerma and absorbed dose rates in an instrument are almost equal.

b. Dose equivalent

In environmental monitoring the quantity generally reported is the **ambient dose equivalent rate (ADER)**, which denotes the energy deposited in a certain material per unit of time, such as tissue. It is calculated from absorbed doses by applying weighting factors. It is expressed in units of sievert (Sv), also 1 Sv = 1 J/kg. The difference between the two is that absorbed dose (Gy) quantifies a physical effect, while equivalent dose (Sv) a biological one. Since this generally cannot be measured, the ADER has been introduced as an 'operational quantity': the dose per unit time in the so-called ICRU sphere, which serves as human 'phantom', i.e., mimics the human body. The actual ADER quantity is dH*(10)/dt, in units of nSv/h, where (10) refers to the dose 10 mm deep within the ICRU sphere (ICRP, 2007):

> The ambient dose equivalent, H*(10), at a point in a radiation field, is the dose equivalent that would be produced by the corresponding expanded and aligned field in the ICRU sphere at a depth of 10 mm on the radius vector opposing the direction of the aligned field.

Detectors are calibrated to the ambient dose equivalent, which is believed to be a conservative estimate of the true (but non-measurable) dose in tissue caused by external radiation. Calibration means that given an exposure, the instruments show the dose value which the ICRU sphere would receive in 10 mm depth. Dose depends on the energy spectrum of the radiation to which matter or tissue is exposed. Since detectors do not react entirely uniformly to radiation of different energy, they are calibrated by irradiation with defined energy.

Additional information on calibration

For European ADR networks, irradiation with ^{226}Ra sources has been recommended for calibration. ^{226}Ra decay products, which contribute most to the gamma radiation of ^{226}Ra sources, simulate quite well the gamma ray spectrum of natural exposure and the one to typical reactor accident fallout. However, also ^{137}Cs and (rarely) ^{60}Co are used for calibration to ADER. For typical environmental radiation, a ^{226}Ra (+progeny) or ^{137}Cs source, kerma dose in air of 1 Gy corresponds to ADER approximately 1.2 Sv H*(10); see also Yi et al. (1997). For further information on this subject, see e.g. IAEA (2000) and ICRP Publication 103, Annexes B3 and B4 (ICRP, 2007).

4.2.2 Components of the ambient dose rate signal and its decomposition

The recorded ADR signal has a number of components, schematically visualised in Figure 4-3.

1. Intrinsic background (also called self-effect) of the instrument: radioactivity of technical components and electronic noise;
2. Cosmic radiation; see Chapter 8;
3. Terrestrial natural radiation:
   a. Gamma rays emitted by primordial natural radionuclides and their progeny in the ground; see Section 4.1 and Chapter 3.
   b. Gamma-radiating radionuclides generated by induced nuclear reaction of cosmic rays.
4. Terrestrial artificial radiation: gamma rays emitted by artificial radionuclides in and on the ground. These are radionuclides from global fallout (from atmospheric nuclear bomb testing) and, concerning Europe, from fallout due to the reactor accident at the Chernobyl nuclear power plant on 26 April 1986. The radionuclide which contributed to ADR over long term is ^{137}Cs (with a half-life of 30 years), for both global and Chernobyl fallout (De Cort et al., 1998). Up to a few years after the Chernobyl accident, other radionuclides also contributed, such as ^{134}Cs (half-life of 2.1 years), ^{106}Ru (half-life of 372 days) and ^{131}I (half-life of 8 days).
5. Airborne natural radiation:
   a. ^{222}Rn and ^{220}Rn which are members of the ^{238}U and ^{232}Th decay series, respectively, are exhaled from the ground into the atmosphere, where they further decay, e.g. into gamma-radiating isotopes of lead and bismuth. These gamma rays are recorded by the ADR monitors. Their intensities depend on the vertical distributions of radon progenies in the atmosphere, which in turn depend on meteorological conditions. A ^{222}Rn concentration of 10 Bq/m^3 in the near-ground atmosphere contributes approximately 2.5 nSv/h to ADER (details and references in Bossew et al. 2007; see also Section 2.2.4).
   b. During precipitation (rain, snow, fog), radon progenies are transported to the ground by scavenging and washout by raindrops. Concentrated on the ground surface, they can give rise to high ADR peaks, which last a few hours and can even trigger radiation alarms.
   c. Cosmic radiation can induce nuclear processes in atoms (mainly oxygen, nitrogen and carbon) present in the atmosphere and generate so-called cosmogenic gamma-radiating radionuclides such as ^{7}Be. Their contribution to ADR is small, far below pSv/h. It varies with the intensity of cosmic rays (see Chapter 5).
   d. In analogy with (b), the cosmogenic radionuclides can precipitate to the ground and thus enhance ADR. This is also a small effect, contributing fractions of nSv/h to ADER.
6. Airborne artificial radiation: After nuclear explosions and accidents, high concentrations of gamma radionuclides can be found. Shortly after the Chernobyl accident, up to several µSv/h were registered in Central Europe, i.e. two orders of magnitude above the usual background radiation.
7. Contamination of the monitor: Airborne natural and artificial radionuclides will be deposited on the housing of the detector and contribute to the ADR signal. Experiments have shown, however, that this effect is small and does not lead to undue bias.
8. Particular signals can arise from nearby activities involving nuclear methods, typically such as material testing using gamma-ray sources. Such cases have occurred, sometimes causing confusion to network operators who may suspect a radiation accident. Lightning may also induce noticeable detector response.
9. Spurious signals: Apart from signal loss, system malfunction may lead to spurious, highly anomalous readings. Usually, these are easy to identify and then to discard.

To estimate the terrestrial natural component, one should subtract all the components listed above except 3a from the ADR.

4.2.3 Variability of natural terrestrial dose rate

Terrestrial dose rate is subject to spatial (i.e. geographical) and temporal variability.

a. Spatial variability

The sources of natural terrestrial gamma radiation are the primordial radionuclides and progeny. Their geographical distribution is not uniform, but varies according to geology and geochemistry, as explained in detail in Section 4.1.

b. Temporal variability

At first glance, it may seem surprising that observed natural terrestrial ADR is not constant over time. The reason is that gamma rays from the source, which are the radionuclides in the upper few tens of centimetres of the ground are attenuated by the matter between emitter and monitor. This attenuation depends on soil humidity: in wet soil, gamma rays are attenuated more strongly than in dry soil.

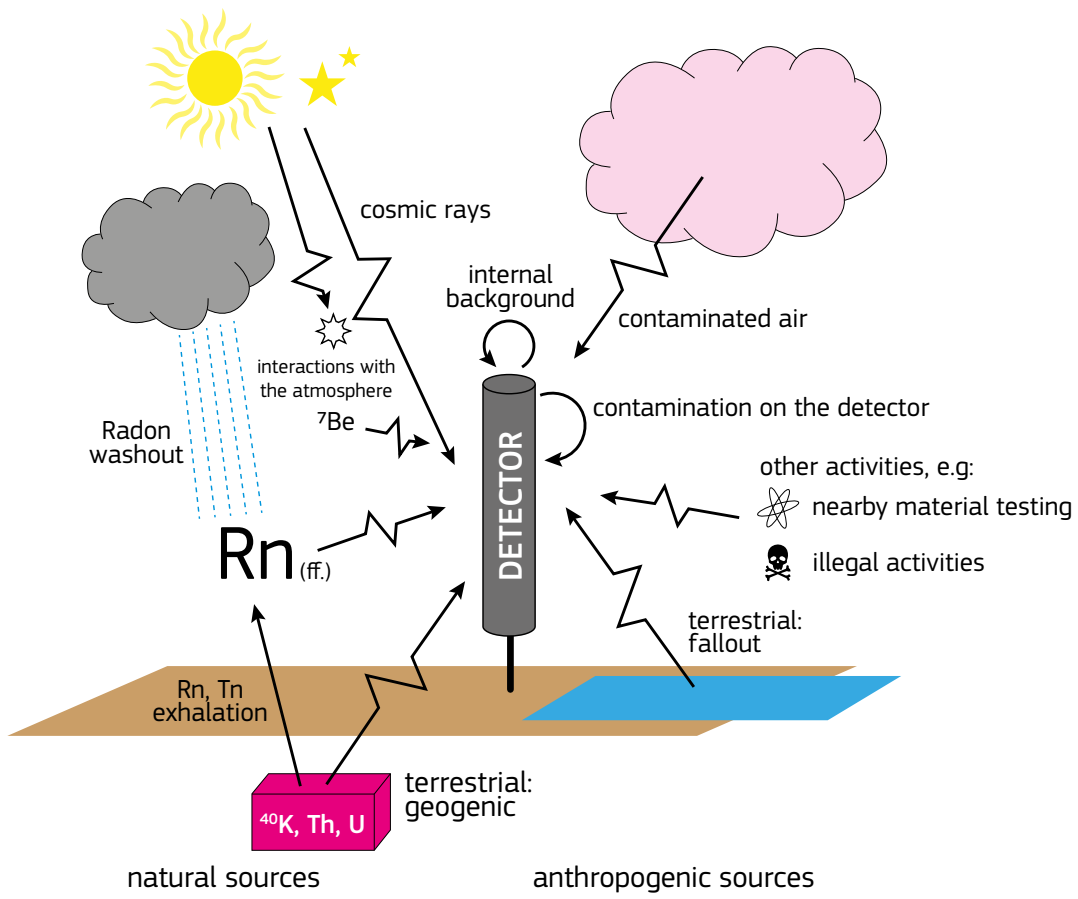

Figure 4-3.
Contributions to the dose rate recorded by a detector. Rn - radon (^{222}Rn), Tn - thoron (^{220}Rn); see Section 2.2.2 for details.
Source: Graph created by Peter Bossew.

Case study: ADER 'rain peaks' due to radon progeny

After a hot and dry period in Vienna, heavy thunderstorms started in the evening of 2 May 2018. The ADER 'rain peak' due to radon progeny precipitated to the ground is clearly visible in Figure 4-4 to the right. The progeny are short-lived (half-lives of about half an hour) and decay within a few hours. ADR returned to background values, but slightly, about 5 nSv/h, lower than before rain, about 93 instead of 98 nSv/h. The reasons are attenuation by the now wet soil and the 'clean' atmosphere, comparatively devoid of radon progeny.

The effect shown in Figure 4-4 is thus a combination of soil humidity and decreased airborne radionuclide concentration. Identification of the individual contributions is rather complicated without dedicated measurements.

A similar effect is shown in Figure 4-5, an ADER series recorded over 4.4 years at a high-lying mountain station in the Austrian Alps. Here the attenuation effect by snow (up to several metres deep at that location) can be observed, which reduces the 'summer background', without snow, from about 80 to 20 – 50 nSv/h. The values are net ADER, i.e. contributions from cosmic rays and self-effect subtracted.

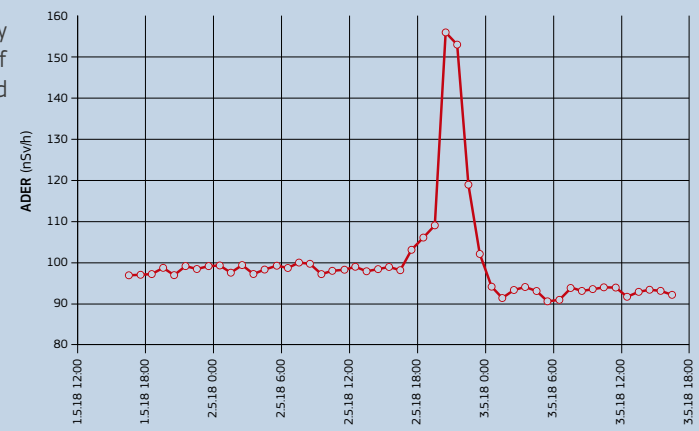

Figure 4-4.
ADER recorded by a monitoring station in Vienna, Austria, around 2 May 2018. Timestamp: UT. The peak is caused by radon progeny deposited by heavy rain after a long dry period.
Source: Graph created by Peter Bossew.

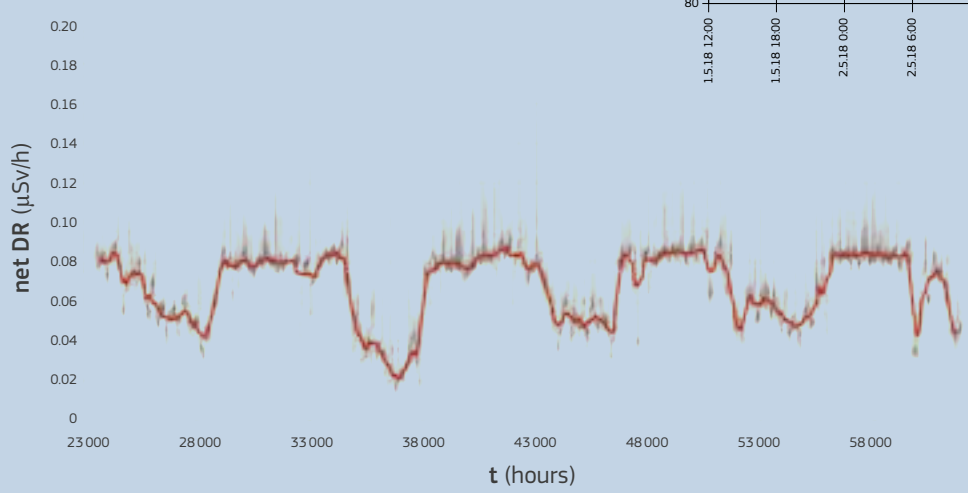

Figure 4-5.
ADER series from a station in the Austrian mountains. Rain peaks and attenuation by snow are clearly visible. Red curve: background after removing the rain peaks.
Source: Graph taken from Bossew et al. (2017).

4.2.4 Variability of dose rate from nuclear fallout

Since this Atlas focuses on natural sources of radiation, the artificial ones, i.e, nuclear fallouts, are only briefly mentioned. Its spatial variability is due to geographically variable fallout density. Global fallout is mainly correlated with long-term precipitation and a latitude effect. The Chernobyl fallout was governed by the movement of the air, which was contaminated when passing the still emitting reactor, and deposition, which mainly depended on precipitation during passage of contaminated air. Maps of Chernobyl fallout can be found in De Cort et al. (1998).

Concerning temporal variability, fallout gamma-ray intensity above ground decreases with radionuclide physical decay; by migration of the contaminant into deeper soil layers and resulting higher attenuation by overlaying soil; and the attenuation effect described. Typically, caesium migrates downwards by a few millimetres per year (Bossew & Kirchner, 2004; Strebl et al., 2009).

The Compton scattered flux has been neglected in this simple model. Its contribution increases with the depth of the source in soil. The dose rate is constituted by scattered and unscattered flux.

Technical details:

Assume that ^{137}Cs (with energy 662 keV) is distributed in soil according to Equation 4-3, which approximates the solution of the diffusion-advection equation. The advection velocity v and dispersion constant D were set to v=0.2 cm/a and D=0.2 cm²/a, respectively, which is realistic. The unscattered gamma-ray flux is given by Equation 4-4, where φ_z denotes the flux from an infinitely thin disk at depth z. In Equation 4-5, C_a, set to unity, denotes the total inventory (Bq/cm²), Y the emission probability (=0.85 for ^{137}Cs), h the measurement altitude above ground (1 m), μ_a the attenuation constant of air (0.0093 m^{-1} for 662 keV), μ_s the attenuation constant of soil and ρ_s soil density, assumed to be 1 g/cm³. (μ_s/ρ_s)=0.075 cm²/g for 662 keV photons. E_1 is the exponential integral of first order.

$$f(z) = \frac{1}{\sqrt{Dt}} \exp\left[-\frac{(z-vt)^2}{4Dt}\right] \quad (4\text{-}3)$$

$$\varphi = \int_0^\infty \varphi_z f(z)\,dz \Big/ \int_0^\infty f(z)\,dz \quad (4\text{-}4)$$

$$\varphi_z = \frac{C_a Y}{2} E_1\left[h\mu_a + z\frac{\mu_S}{\rho_S}\rho_S\right] \quad (4\text{-}5)$$

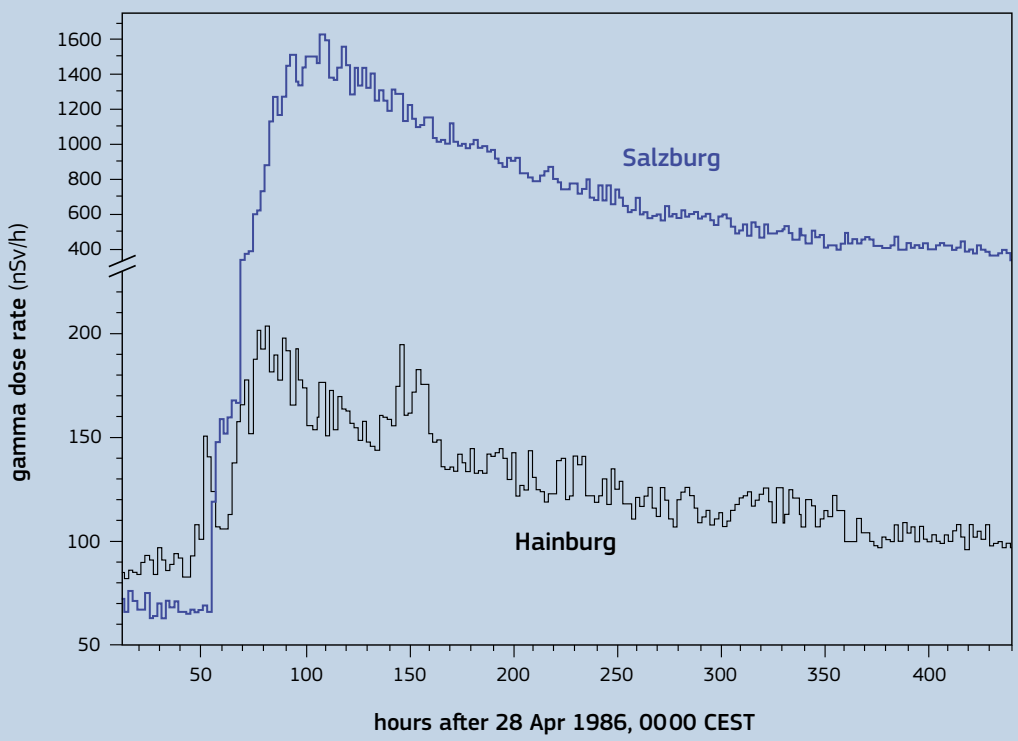

Figure 4-6.
Dose rate signal after the Chernobyl accident recorded by two stations of the Austrian early-warning network. Temporal resolution: 2 hours. Please note the gap in the y-axis.
Source: Graph created by Peter Bossew.

Temporal changes in dose rate, ^{137}Cs concentration and gamma-ray flux after the Chernobyl accident

Figure 4-6 shows ADER values recorded at two Austrian monitoring stations after the Chernobyl accident on 26 April 1986. Except for the beginning, the dominant part of ADER is caused by radiation from radionuclides deposited on the ground, although airborne concentrations were also partly quite high. The peak in the Hainburg series at about t=150 h may have been caused by the passage of another contaminated cloud. The decrease in ADER reflects the decay of short-lived radionuclides such as ^{132}Te and ^{131}I.

Temporal change of the depth distribution of ^{137}Cs concentrations in soil at a location in Salzburg (Austria) is shown in Figure 4-7 (each curve represents the mean of 3 soil profiles). One can recognise decreasing ^{137}Cs concentration in the surface layer and the shift of the maximum towards deeper layer; both effects result from migration, typically in the order of a few millimetres per year. Also the total activity decreases (represented by the areas under the curves), due to physical decay and migration to deep soil layers that have not been sampled, and into ground water.

During the first days to weeks after the Chernobyl accident, dominant radionuclides, which contributed most to the ambient dose rate, were iodine and tellurium isotopes. Due to their short half-lives (for ^{131}I, 8 days) their contribution soon disappeared. For months to a few years, radionuclides such as ^{134}Cs, ^{106}Ru, ^{125}Sb and ^{144}Ce contributed to the dose rate. Today (2019), more than 33 years after the accident, only the long-lived ^{137}Cs (with a half-life of 30 years) can be detected. Long-lived radionuclides such as ^{90}Sr and plutonium isotopes are present and can be measured, but since they do not emit gamma rays, they do not contribute to ambient dose rate.

According to the changes of total inventory and depth distribution of the contaminant, the gamma-ray flux above ground also changes with time. An example is shown in Figure 4-8.

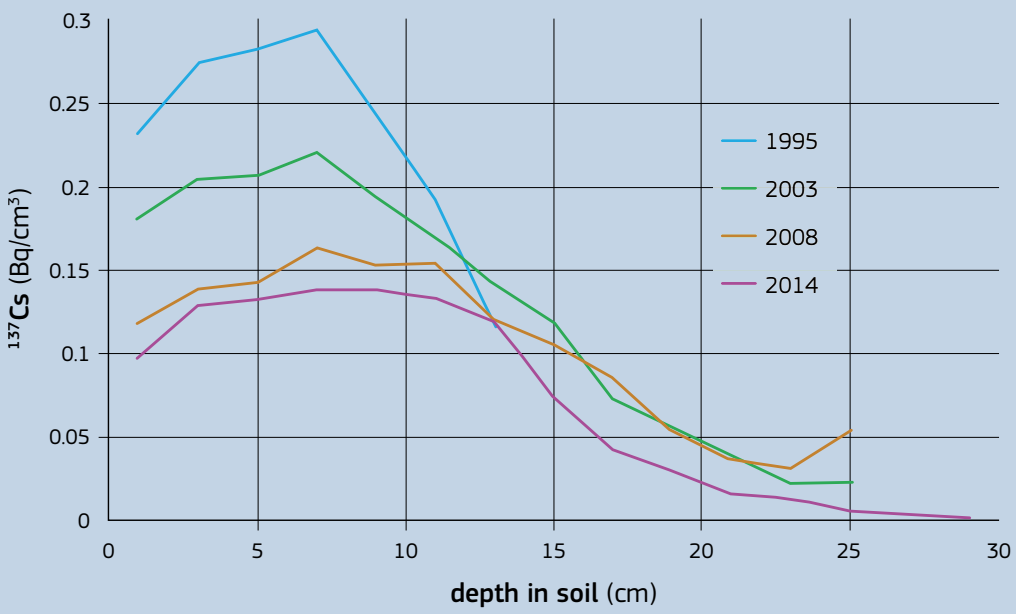

Figure 4-7.
Changes of the depth distributions of ^{137}Cs in Salzburg, Austria, from 1995 to 2014.
Source: Data: courtesy H. Lettner.

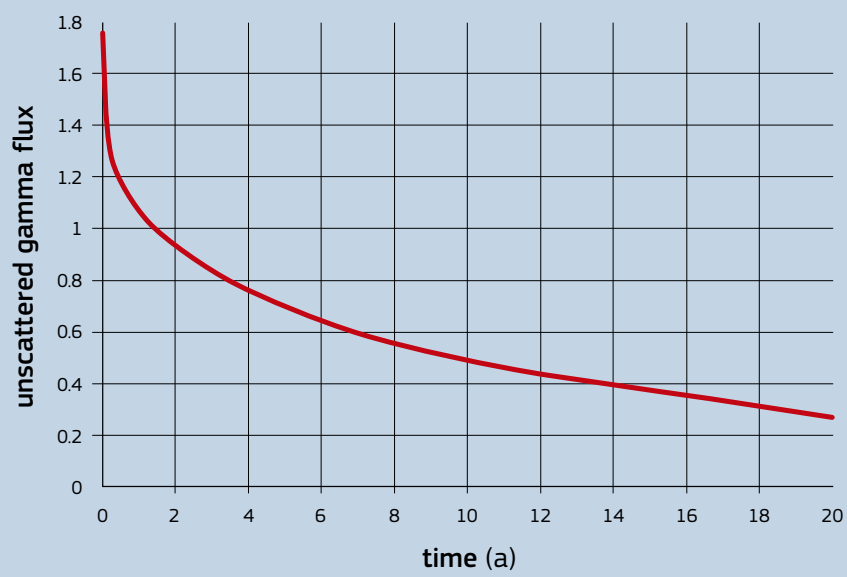

Figure 4-8.
Time dependence of the unscattered 662 keV gamma-ray flux, 1 m above ground over a normally distributed ^{137}Cs source in the soil.
Source: Graph created by Peter Bossew.

4.3 Materials and methods

Terrestrial gamma dose rate can be determined experimentally by measurement or indirectly by using geochemical data.

Geophysical field radiometric measurements, focused on radioactivity of rocks and soils and backed with sophisticated specialised instruments, developed techniques of data acquisition and data processing, can provide reliable information on the dose rate and contents of radioactive elements in extensive areas. Geophysical radiometric gamma surveys are conducted as a total count measurement (TC) or gamma-ray spectrometry, both applicable for the airborne, car-borne and ground measurements with portable radiometric instruments.

4.3.1 Dose rate in geophysical research

Total count rate measurement

Total count (TC) surveys with count rate meters equipped with scintillation detectors or Geiger-Müller counters are mostly applied in ground measurements. The relationship between the recorded count rate, n_{TC} (counts per second or cps), and the concentration of K, U, and Th in rocks is given by

$$n_{TC} = s_K c_K + s_{Th} c_{Th} + s_U c_U + n_{BG} \quad (4\text{-}6)$$

where:
s_K, s_{Th}, s_U are the sensitivities of a TC radiometric instrument (cps per unit concentration of relevant radionuclide) for K, Th and U, respectively; and
c_K, c_{Th}, c_U are K, Th and U element concentrations.

Sensitivities of the instrument can be estimated by measuring the TC response over calibration pads or over selected geological bodies that have different K, Th and U concentrations (IAEA, 2003). The background count rate, n_{BG}, is estimated by measuring over a large water plane. The count rate response of the TC instrument to gamma radiation of K, Th and U of specific energy fundamentally depends on the type of detector and its detection efficiency (IAEA, 1976), and on the energy discrimination threshold of the instrument. The results of a TC measurement can be expressed in dose rate (nGy/h), by converting count rates n_{TC} to dose rate using the instrument calibration constant. Since the response of a TC instrument significantly depends on its detector and energy discrimination threshold, the resultant dose rates of single instruments may deviate from correct values. Reference literature describes these effects and range of deviations over rocks having variable proportions of K, Th and U (e.g. IAEA, 1990; IAEA, 2003; IAEA, 2013; Matolin, 2017).

Gamma-ray spectrometry (see also Section 2.5)

Since the 1960s, gamma-ray spectrometry has been widely used for geological surveys and environmental monitoring since the 1960s. Field multichannel scintillation gamma-ray spectrometers record count rates (cps) in energy intervals which are centred on the 1 461 keV (^{40}K), 1 765 keV (^{214}Bi, decay product of ^{238}U) and 2 615 keV (^{208}Tl, decay product of ^{232}Th) photopeaks for estimating the K, Th and U concentrations, respectively (IAEA, 1989). The K, Th and U energy window count rates, n_i, (cps), recorded in three selected energy windows i = 1, 2, 3, are linearly related to the K, Th and U concentrations c_j, j = K, Th, U such that

$$n_i = s_{iK} c_K + s_{iTh} c_{Th} + s_{iU} c_U + n_{iBG} \quad (4\text{-}7)$$

The sensitivity constants, s_{ij}, are estimated from measurements on the four calibration pads of a calibration facility, or for the airborne gamma-ray spectrometer by flying over a calibration strip (Tauchid & Grasty, 2002). Background activity can be estimated by taking measurements over a large body of water. For a given count rate n_i that is corrected for background, the radioelement concentrations c_K, c_{Th}, c_U can be calculated using either a matrix or stripping method. More sophisticated methods based on the full gamma-ray energy spectra processing have also been developed (IAEA, 2003).

Scintillation detectors with NaI(Tl) crystals, having relatively high detection efficiency, are mostly used for airborne, car-borne and ground radiometric mapping. High-purity germanium (HPGe) semiconductor detectors (see details in Section 2.5.3), with high energy resolution but low detection efficiency resulting in long exposure times, are used for gamma-ray spectrometric identification of unknown radionuclides and investigation of already localised radiation sources.

Methods of field gamma-ray spectrometry

Airborne gamma-ray spectrometry is an efficient technique to cover extensive areas. Specific features of airborne gamma-ray spectrometry include large-volume scintillation detectors of 30 – 50 litres NaI(Tl), additional upward looking 4 l NaI(Tl) detector for atmospheric radon correction, a multichannel pulse amplitude analyser, an energy spectrum stabilisation and dead time correction unit. Additional instruments are radar altimeter and differential GPS. Measurements are carried out at constant heights above the ground, selected in the interval 30 – 120 m, along parallel flight lines, with flight speed between 25 – 50 m/s (90 – 180 km/h), and with a sampling interval of 1 s. The field of view (zone of influence) is usually related to the diameter, d, of a circular plane, which generates an assigned percentage (%) of radiation from an infinite source. The field of view is a function of the flying height h. Processing of airborne gamma-ray data requires a number of corrections (IAEA, 1991; IAEA, 2003).

A NaI detector placed one metre above the ground.
Source: Laura Tositti.

Car-borne gamma-ray spectrometry is applicable in natural car-accessible terrain. Specific features of car-borne measurements are the use of 4 – 8 l NaI(Tl) scintillation detectors, car speeds of 15 – 30 km/h, and sampling intervals of 1 – 4 s. The field of view for a rooftop-mounted detector may be in the range of 14 – 36 m.

Ground radiometric measurements with portable total count instruments or portable gamma-ray spectrometers can be performed in stationary mode or dynamic mode. Portable gamma-ray spectrometers are equipped with 103 – 350 cm^3 NaI(Tl) scintillation detectors, or recently also with BGO crystals, $LaBr_3$ and other crystals (see Section 4.3.4). Uniformity of ground radiometric measurements requires a fixed height of the detector over terrain. For a detector placed on the ground, the detected gamma radiation comes from the circular area with a diameter of about 1 m. As the detector is raised from the ground, the field of view increases progressively. Stationary gamma spectrometry measurements require sampling times of 2 minutes over rocks of enhanced radioactivity (granites) and 6 minutes over low-radioactivity rocks (limestone). With HPGe detectors, typical sampling times are in the order of several tens of minutes.

Calibration of radiometric instruments

Calibration of radiological radiometric instruments in open air is mostly performed by means of suitable point reference sources (standards), as are ^{226}Ra, ^{137}Cs, or others. Calibration of geophysical field radiometric instruments used for radiometric mapping and environmental studies is conducted by means of calibration pads. A calibration pad is a three-dimensional slab of concrete containing a known concentration of natural radioelements K, Th and U. A calibration pad should simulate a geological source by its geometry, radionuclides, matrix composition, density, humidity and generated gamma ray energy spectrum. The objective of the use of calibration pads is to analyse correctly natural radionuclides K, Th and U in rocks and control existing deviations between registered instrument count rate (cps) and existing dose rate. Only field total count radiometric instrument, having uranium equivalent of potassium equal to 2.30 and uranium equivalent of thorium equal to 0.44, reports correct values of the dose rate (Løvborg, 1984; IAEA, 1990). Three calibration pads individually enriched by potassium, uranium, or thorium, and one low radioactivity background pad have been recommended by the IAEA (1989). A calibration strip of known ground K, Th and U concentration serves for calibration of airborne gamma ray spectrometers. Calibration of gamma ray spectrometers results in determination of instrument sensitivities, s_{ij}, stripping ratios, and background count rates n_{iBG} (IAEA, 2003). Calibration of radiometric instruments is a fundamental procedure for standardisation of radiometric data. The International Atomic Energy Agency under the concept of 'A Global Radioelement Baseline' supports uniformity of radiometric data through using the IAEA primary reference standards for laboratory gamma ray spectrometry (IAEA, 1987), construction and use of three-dimensional calibration pads (IAEA, 1989), calibration of radiometric instruments, and acquisition of field data and data processing by verified procedures (IAEA, 2003; IAEA, 2010). An excellent example of application of the IAEA concept 'A Global Radioelement Baseline' is the compilation of a uniform radiometric map of Australia (Minty et al., 2009). An appreciable assistance in calibration of field gamma-ray spectrometers was the introduction and manufacturing of portable calibration pads (Grasty et al., 1991) that enabled calibration of field radiometric instruments in more countries.

Calibration pads, concrete enriched with K, Th and U.
Source: Peter Bossew.

4.3.2 Dose rate calculation from geochemical data

Computation of terrestrial gamma dose rate (TGDR) using known concentration of natural radioelements K, Th and U in rocks and soils is based on the model of gamma radiation of the homogeneous infinite plane over the Earth's surface. Constants for converting the unit K, Th and U mass concentration in soil at an elevation of 1 m above the homogeneous soil surface cited in literature (IAEA, 2003; Will et al., 2003) differ negligibly, in dependence on selected density of rocks and applied radiation constants.

A possible approach for estimating the TGDR, i.e. the external doses due to natural radionuclides, is a theoretical calculation based on concentrations of natural radionuclides in the soil (UNSCEAR, 2008).

In particular, the TGDR is estimated from the concentrations of all the natural radionuclides in the soil, considering all their gamma emissions. In doing so, a fundamental assumption has to be made: the secular radioactive equilibrium (see Section 4.4.2). Apart from ^{40}K, the large majority of the terrestrial radionuclides in soil emitting gamma rays belongs to the uranium and thorium series, two large groups of radionuclides produced by the decay of uranium and thorium. The parents of these natural families, namely ^{232}Th ($T_{1/2}$=1.41·10^{10} years) and ^{238}U ($T_{1/2}$=4.47·10^{9} years), are very long-lived radioisotopes, with half-lives in the order of billions of years, much longer than those of all the other radioisotopes belonging to the series. As a consequence of that the so-called secular radioactive equilibrium condition is established between the members of the radioactive families: i.e. the activity of all the radionuclides have the same value, thus drastically simplifying the calculation issue. It is therefore possible to estimate the TGDR simply by knowing the concentration in soil of only three radionuclides: ^{40}K, ^{232}Th and ^{238}U.

Several methods can be used to calculate the gamma dose rate, starting from the gamma-ray flux produced by radionuclides. In most applications, the gamma-ray transport equation is solved by using Monte Carlo techniques. However, for the TGDR, a simplified semi-analytical approach, namely the point-kernel isotropic method, can be successfully used. In this case, the soil is modelled as a semi-infinite space, and the dose rate is evaluated at a receptor point, 1 metre above the ground. Each infinitesimal volume (dv) of soil, acting as a point source irradiating isotropically, gives at the receptor point an infinitesimal gamma-ray fluence dΦ whose expression is:

$$d\Phi = \frac{e^{-(\mu/\rho)_s \cdot \rho_s \cdot r_s + (\mu/\rho)_a \cdot \rho_a \cdot r_a} dS}{4\pi r^2} \qquad (4\text{-}8)$$

where:
dS is the intensity of the gamma source due to the presence of gamma-emitting radionuclides in the infinitesimal volume of soil dv;
$(\mu/\rho)_s$ and $(\mu/\rho)_a$ are the mass attenuation coefficients for the photons in soil and air respectively; and
ρ_s and ρ_a are the soil and air density while r is the length of the total path travelled in the medium (soil+air: $r=r_s+r_a$) by the gamma rays from soil to the receptor point.

The corresponding, absorbed dose rate at the receptor point can thus be evaluated integrating Equation 4-8 over the semi-infinite volume V, as follows:

$$\dot{D} = \int_V \frac{k \cdot E \cdot \left[\frac{\mu_{en}}{\rho}\right] \cdot B \cdot e^{-(\mu/\rho)_s \cdot \rho_s \cdot r_s + (\mu/\rho)_a \cdot \rho_a \cdot r_a} dS}{4\pi r^2} \qquad (4\text{-}9)$$

where:
E is the photon energy;
(μ_{en}/ρ) is the mass energy absorption coefficient in air at the point dose;
k is an appropriate conversion factor; and
B is the build-up factor, i.e. the parameter that quantifies the dose due to the scattered photons.

Another key element in Equation 4-9 is the quantity dS, which is directly related to the gamma-emitting radionuclides in soil. The explicit expression for dS is:

$$dS = \sum_j \left(\sum_k a_j \cdot y_{jk} \right) \cdot dv \qquad (4\text{-}10)$$

where:
a_j is the volumetric activity concentration (Bq/cm^3) of the generic radionuclide j;
y_{jk} is the yield of the j_k gamma emission of the radionuclide j; and
dv is the infinitesimal volume of soil.

Equation 4-10 is then inserted into Equation 4-9 and the TGDR can thus be computed. In doing so, Equation 4-9 has of course to be evaluated for each generic gamma line j_k, with given energy E_{jk} and with their corresponding values for the attenuation and absorption coefficients: $(\mu/\rho)_{sjk}$, $(\mu/\rho)_{ajk}$ and $(\mu_{en}/\rho)_{jk}$.

Operating in this way, in 1972 Beck and co-workers (Beck et al., 1972) were able to calculate the TGDR due to natural radioactivity. They proposed a very a simple formula:

$$TGDR(nGy/h)) = 0.0424 \cdot C_K + 0.668 \cdot C_{Th} + 0.431 \cdot C_U \qquad (4\text{-}11)$$

where:
C_K, C_{Th} and C_U are, respectively, the activity concentration of ^{40}K, ^{232}Th and ^{238}U in Bq/kg.

More recently, following a very similar approach, the UNSCEAR (UNSCEAR, 2008) has proposed a slightly different formula, based on newer data:

$$TGDR(nGy/h)) = 0.0417 \cdot C_K + 0.604 \cdot C_{Th} + 0.462 \cdot C_U \qquad (4\text{-}12)$$

The latter expression is used to calculate the European Terrestrial Gamma Dose Rate Map (see Section 4.4.2): the dose rate can be evaluated in each cell grid simply by inserting in the above equation the corresponding ^{40}K, ^{232}Th and ^{238}U activity concentration values (Bq/kg).

The use of expressions such as Equation 4-9 and its simplified forms (Equation 4-11 or 4-12) for evaluating the TGDR are based on some important underlying assumptions that are worth discussing in some detail. These fundamental assumptions are:

- The secular radioactive equilibrium condition between all the members of the radioactive families (Th and U), already mentioned in the introduction; this is a very important assumption, allowing the calculation of the TGDR from the simple knowledge of the activity concentration of only three radionuclides: ^{40}K, ^{232}Th and ^{238}U. It is almost everywhere a very good assumption, but some local exceptions generally cannot be ruled out.
- The complete homogeneity of the soil medium, characterised by a unique density value ρ_s, a unique mass attenuation coefficient $(\mu/\rho)_s$ and a standard composition, valid for all types of soils.

4.3.3 Dose rate in the EURDEP system

Motivation and history

a. Introduction

Many countries operate automatic systems, which continuously monitor radiometric quantities in the environment. Their purpose is to warn against effluents of large-scale radiological emergencies, which might have been caused by reactor accidents. Most monitoring stations measure ambient dose rate, while a smaller number collect air samples and measure activity concentrations of airborne radioactivity. While the systems are operated and evaluated nationally, a large part of data generated in European countries is transmitted to the European Radiological Data Exchange Platform (EURDEP), which makes radiological monitoring data from most European countries available in nearly real-time. While participation of the EU Member States is regulated by EU law, non-EU countries take part on a voluntary basis. As of mid-2019, 39 countries participate to EURDEP. In addition to EU Member States and non-EU countries, a few non-European countries have joined. Extensive information about EURDEP is available on its website, https://remon.jrc.ec.europa.eu/. The values are displayed as maps; see Figure 4-9 as an example.

More than 5 000 stations across Europe monitor ambient dose rate (ADR); and a few tens of stations, radionuclide concentrations in air. (Data transmission from the latter is currently poor.)

Large-scale nuclear accidents or events are fortunately rare. Indeed, since the Chernobyl accident (on 26 April 1986), no anthropogenic event extending beyond one station has been monitored. (Such events are usually material tests using gamma radiation sources.) The Fukushima accident (e.g. Masson et al., 2011; Bossew et al., 2012) did not lead to a detectable increase of ADER in Europe. Such events are only detectable by air monitoring.

A secondary use of dose rate monitoring stations is the assessment of natural radiation. Operating continuously, these monitors generate large amounts of 'background' data, which are being stored by national authorities as well as by the Joint Research Centre of the European Commission. The data can potentially be used to assess and map natural environmental radioactivity, which is why they are discussed in this Atlas.

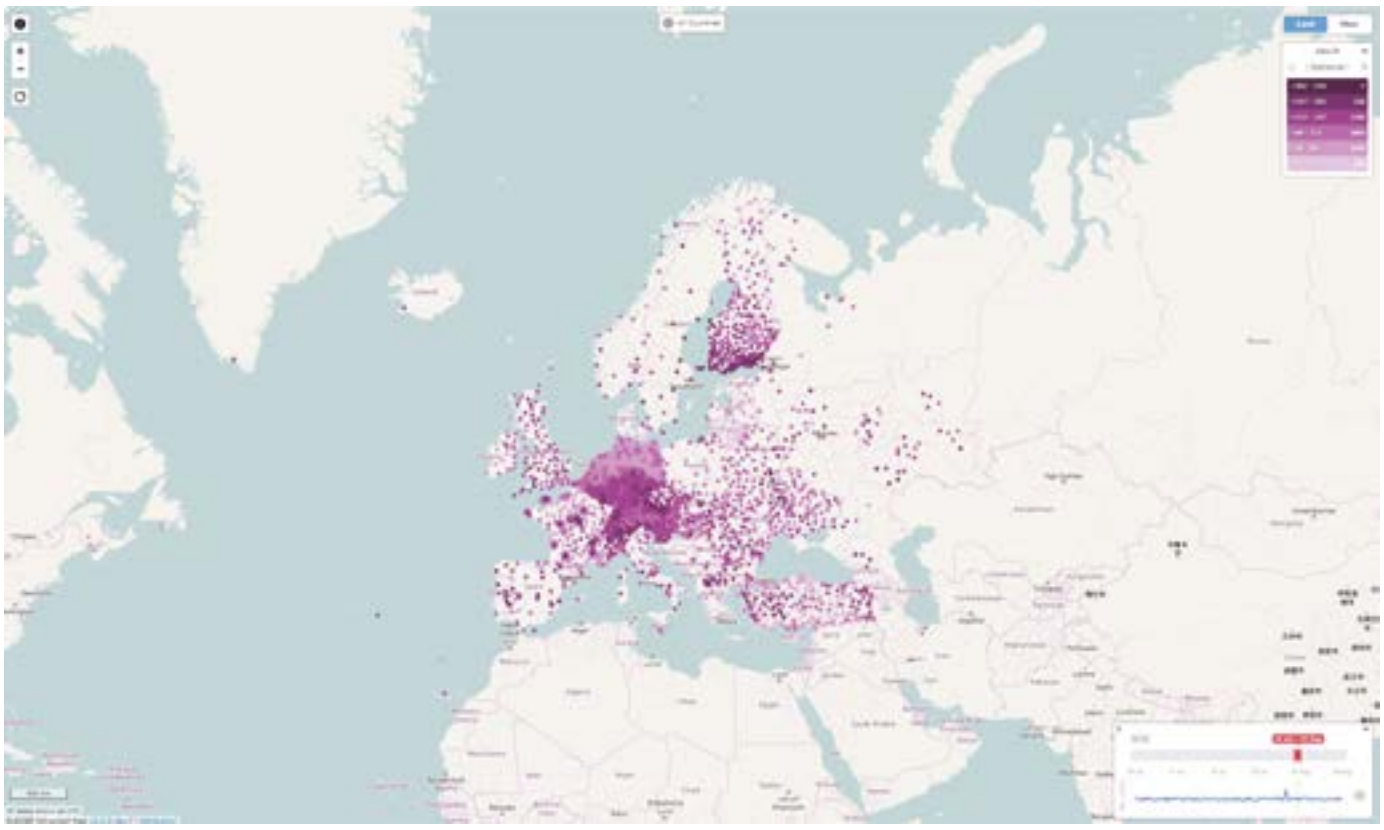

Figure 4-9.
EURDEP screenshot. ADR stations, showing the arithmetic means of ADER (H*(10), nSv/h) over one day, ending on 1 August 2019.
Source: EURDEP, EC-JRC, 2019.

b. Radiation background and signals

Except for the Austrian network that was operable during the Chernobyl accident, no new artificial contamination (i.e. on top of existing) has been observed by EURDEP. In Europe, the ADR due to contaminated air from the Fukushima accident was about three orders of magnitude smaller than typical detection limits of the dose rate monitors. Air contamination could be easily measured with high-volume laboratory-based air samplers, but not by automatic air sampling stations.

This means that the ADR readings represent natural radiation as well as existing residual fallout. Over most of Europe, the latter component contributes a few percent at most, with about 10% in regions highly affected by Chernobyl fallout (parts of Scandinavia, Austria, South Germany and others). An exception is one station in Southeast Belarus, where the signal is dominated by Chernobyl fallout.

In ADR readings, natural and artificial components cannot be distinguished. Estimating the latter depends on gamma-spectrometric measurements, which require instruments that are more complicated and expensive than the relatively simple ADR monitors.

As mentioned, although made for detecting large-scale accidental contamination, the systems constantly generate background signals, which however convey interesting radiometric information. Therefore, in recent years, effort has been made to better understand these signals and possibly exploit them for scientific and general radioprotection purposes.

Network policy and design

Radioactivity monitoring networks are usually designed for two main purposes: to detect anomalies for early warning and to manage accidents. In the first case, monitoring stations are located preferentially around nuclear installations and/or, if neighbouring countries have nuclear power plants, at country borders. The preferential siting of monitoring stations requires that the potential sources of radioactive releases are known in order to maximise the probability of detecting local anomalies and report these in the shortest possible time. Fixed station monitoring is therefore not capable of warning against, or monitoring small-scale nuclear events, in particular not malevolent criminal and terroristic activity.

History has shown, however, that large-scale disasters can occur and, should the radioactive release be atmospheric, that contamination can affect a whole continent. The management of such an accident would ideally require radiation levels to be reported anywhere at any time. Following the Chernobyl accident (on 26 April 1986), most countries have set up an additional number of automatic stations spread over their territories and/or at critical places (typically large cities), even when these places were distant from any nuclear power plant.

The map of monitoring networks shown in Figure 4-9 easily illustrates the above: while in some countries, a number of stations seems to be distributed randomly over the territory, aggregated stations will, in most cases, reflect sites of nuclear industry. Inversely, a lower density of stations will usually indicate regions with lower population density and regions where physical obstacles such as water bodies and mountains make it difficult to install and maintain a monitoring station.

Test probes at the BfS premises in Berlin, showing antennas in various stages of development. Each can be equipped with a pair of Geiger-Muller counters. one for low and one for high dose rate.
Source: Peter Bossew.

Thus, the siting criteria for the monitoring stations, the density of the monitoring network and the spatial distribution of individual stations depend on many factors, including:

- The intensity of the nuclear activity within the country;
- The country's economic resources that are available for acquiring and maintaining a monitoring network;
- Environmental policies and regulations;
- Concern about nuclear activities of neighbouring countries;
- The importance which is attributed to a network's capability to provide a detailed geographical picture of an existing contamination situation;
- The geographical distribution of the population and of the main resources of the country; a certain relationship between network and population densities can be observed, see Figure 4-10.
- Topography.

What is shown here as stations of a national network is actually a collation of several networks, in some cases, where clustered stations around nuclear power plants are part of a network operated by an authority different from the one responsible for the sparse networks that cover much larger areas.

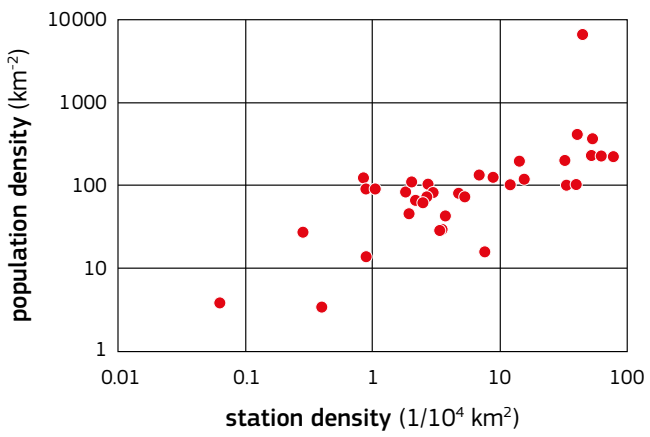

Figure 4-10.
Scatterplot of station density vs. demographic density. The outlier in the upper-right corner represents Hong Kong.
Source: Graph created by Peter Bossew.

However, because of the need for managing the collected data for early-warning coherently and for the longer term, there is a trend in combining all networks under the umbrella of a single national authority to ensure better coordination (see e.g. Deurwaarder et al., 2001) in case of an accident. Here we consider all stations as part of a single network.

Figure 4-9 clearly shows that the geographical distribution of stations is not uniform between countries. This reflects different policies which underlie the networks, as discussed above. Some countries attempt to cover their territories more or less uniformly to be able to identify fallout levels as quickly as possible and to be able to follow dispersing contaminated air; examples are Germany, Austria, Belgium, Turkey or the UK. Others chose to locate stations more densely around nuclear plants (e.g. France and Spain). Yet others locate stations preferentially along borders to detect radioactive clouds intruding from abroad as efficiently as possible (the East coast of Ireland, Turkey). In Finland, the station density conforms approximately to the population density.

Apart from geographical configuration of the network, countries choose different station densities. This reflects the desired degree of precision of geographical information generated by the monitor readings. Evidently, higher precision conflicts with economic constraints and a suitable trade-off has to be found.

As a consequence of the geometrical heterogeneity, when used for mapping on European level, different degrees of precision between regions must be accepted.

Photo taken during a art.35 Euratom Verification visit in Croatia, September 2013, showing various types of detector for environmental radioactivity.
Source: Tore Tollefsen.

Network design: Description of network geometries

Figure 4-9 shows the monitoring stations of the European network, excluding the Atlantic islands, that are transmitting data as of June 2019.

The network patterns, or 'geometries', are evidently different between countries, reflecting different policies, as discussed above. Basic statistics of network geometries are given in Table 4-2, where:

- CE is the Clark-Evans index of complete randomness. CE=1 indicates that the distribution of stations is compatible with a random distribution; CE<1 means that the pattern is aggregated or clustered; CE>1, that it is more dispersed that could be expected for a random pattern.
- D2 is the fractal correlation dimension that quantifies 'patchiness' of the network. A regular or random pattern has D2 = 2, i.e. the 'patchier' it is, the lower is D2. For instance, France and Switzerland have low values of D2, whilst the UK and Norway have high values. Turkey has a uniform pattern inland but clusters along her borders, which reduces D2 somewhat.
- CV is the coefficient of variation of estimated station density. A high coefficient of variation of the estimated station density points to presence of regions with low and high density, notably France, Switzerland and Italy. In France and Switzerland, the reason is a high degree of clustering around nuclear facilities, while in Italy the 'non-stationary' nature of the density function, because density in the North is much higher than in the South of Italy. (The two effects could be distinguished by spatial trend analysis.)
- CV (NND) is the coefficient of variation of the nearest neighbour density, is an indicator of station clustering: Within clusters, NND is smaller than outside, which leads to higher dispersion of the NNDs.

code	country	area (km²)[1]	number of stations	stations per 10 000 km²	km² per station	population density (km⁻²)[1]	AM(NND) (km)	CE index	CV (NND)	corr. dim. D2	SD(D2)	CV(density)[2]
AL	Albania	28 748				100						
AD	Andorra	468	0			165						
AM	Armenia	29 743				101.5						
AT	Austria	83 856	327	39	256	105	10.2	1.27	0.45	1.81	0.05	0.23
AZ	Azerbaijan	86 600				114						
BA	Bosnia and Herzegovina	51 126				74						
BE	Belgium	30 510	160	52.44	191	372	9.1	1.31	0.71	1.4	0.04	0.68
BG	Bulgaria	110 994	27	2.43	4 111	64	45.6	1.42	0.49	1.67	0.08	0.4
BY	Belarus	207 600	40	1.93	5 190	46	55.6	1.54	0.23	2.02	0.09	0.16
CA	Canada	9 984 670	63	0.06	158 487	3.92	172.8	0.87	1.97			
CH	Switzerland	41 290	132	31.97	313	203	10.2	1.15	1	1.07	0.09	1.23
CY	Cyprus	9 251	8	8.65	1 156	126	29.4	1.73	0.6			
CZ	Czech Republic	78 866	54	6.85	1 460	135	21	1.10	0.62	1.87	0.06	0.21
DE	Germany	357 168	1 853	51.88	193	232	9.7	1.40	0.48	1.76	0.01	0.53
DK	Denmark[3]	43 094	11	2.55	3 918	132	71.1	2.27	0.51			
EE	Estonia	45 339	15	3.31	3 023	29	61	2.22	0.34	1.68	0.29	0.26
ES	Spain[4]	505 992	45	0.89	11 244	92						
ES	Spain[5]	493 476	43	0.87	11 476		72.4	1.35	0.62	1.36	0.05	0.58
FI	Finland	338 145	256	7.57	1 321	16	25.3	1.39	0.55	1.75	0.02	0.71
FR	France[6]	557 394	857	15.38	650	118	9.5	0.74				
FR	France[7]	643 801	873	13.56	737							
FR	France[8]	548 714	855	15.58	642		9.3	0.77	1.61	1.01	0.01	0.99
GB	United Kingdom[9]	248 532	93	3.74	2 672		49	1.89	0.36	1.96	0.03	0.48
GE	Georgia	69 700				53						
GR	Greece	131 940	24	1.82	5 498	85	64.2	1.73	0.63	1.9	0.09	0.3
GL	Greenland	2 166 086	2	0.01	1 083 043							
HK	Hong Kong	2 755	12	43.56	230	6 777	10	1.32	0.73			0.29
HR	Croatia	56 594	30	5.30	1 886	73	39.1	1.80	0.61	1.3	0.05	0.55
HU	Hungary	93 030	112	12.04	831	105	12.3	0.85	1.08	1.32	0.07	0.82
IE	Ireland	70 273	15	2.13	4 685	68	64.9	1.90	0.56	1.17	0.18	0.35
IS	Iceland	102 775	4	0.39	25 694	3.4						
IT	Italy	301 338	419	13.90	719	201	14	1.05	0.92	1.49	0.07	1.18
KZ	Kazakhstan	2 724 902				6.49						
LI	Liechtenstein	160	1	62.50	160	233						
LT	Lithuania	65 300	24	3.68	2 721	43	25.6	0.98	0.69	1.24	0.04	0.4
LU	Luxembourg	2 586	20	77.34	129	228	9.2	1.62	0.45			0.36
LV	Latvia	64 589	22	3.41	2 936	30	31.8	1.17	0.81	1.08	0.17	0.39
MC	Monaco	1.95	0	0		18 469						
MD	Moldova	33 846	0	0		103						
ME	Montenegro	13 812	0	0		45						
MT	Malta	316	3	94.94	105	1 410	17.6	3.42				
NL	Netherlands[10]	41 198	166	40.29	248	414	11	1.40	0.39	1.63	0.02	0.33
MK	North Macedonia	25 713	12	4.67	2 143	81	68.8	2.97	0.27	1.99	0.35	0.2
NO	Norway[11]	384 801	34	0.88	11 318	14	122.9	2.31				
NO	Norway[12]	323 779	33	1.02	9 811			1.26	0.27	1.8	0.09	0.29
PL	Poland	312 685	26	0.83	12 026	123	65.8	1.20	0.60		0.06	0.15
PT	Portugal	91 568				112						
RO	Romania	238 392	71	2.98	3 358	82	31.7	1.10	0.86	1.01	0.08	0.71
RS	Serbia[13]	77 453	8	1.03	9 682	91	100.4	2.04	0.26			
SM	San Marino	61	0	0		544						
RU	Russia[14]	3 972 400	111	0.28	35 787	28	62	0.66	0.67	1.2	0.03	0.36
SE	Sweden	449 964				22						
SI	Slovenia	20 273	67	33.05	303	102	9.6	1.10	0.74	1.3	0.03	0.61
SK	Slovak Republic	49 036	10	2.04	4 904	111	35.7	1.02	0.42	1.06	0.08	0.18
TR	Turkey	783 562	211	2.69	3 714	105	42.7	1.40	0.46	1.73	0.03	0.2
UA	Ukraine[15]	603 628	158	2.62	3 820	73.8	45.2	1.46	0.3	1.87	0.05	0.31
VA	Holy See	0.44	0	0		2 273						
XK	Kosovo	10 908	0	0		175						
	Median			**2.98**	**2 721**	**102.5**	**31.8**	**1.37**	**0.6**	**1.56**		**0.36**

1 From Wikipedia
2 Over cells by Gauss kernel estimate; lower 10 % truncated
3 Excluding Faroe Islands (1 399 km²) and Greenland (2 166 086 km²)
4 Including Balearic Islands (4 992 km²), Canary Islands (7 493 km²), Ceuta (18.5 km²), Melilla (12.3 km²)
5 Only mainland, i.e. excluding islands, Ceuta and Melilla
6 Excluding overseas departments
7 Including overseas departments
8 Mainland France = (6) minus Corsica (8 680 km²)
9 Excluding overseas territories, including Jersey (118.2 km²), Guernsey (65 km²), Isle of Man (572 km²), Gibraltar (6.7 km²)
10 Only European territories, i.e. excluding Caribbean territories
11 Including Svalbard (61 022 km²), excluding Jan Mayen (377 km²)
12 Excluding Svalbard and Jan Mayen
13 Excluding Kosovo
14 European part
15 Including Crimea (27 000 km²)

Table 4-2.
EURDEP ADER stations: All European countries as well as Canada and Hong Kong, that contribute data to the network. Based on stations in operation end-May 2018. AM(NND) – Mean nearest neighbour distance; CE – Clark-Evans (see text); CV(NND) – coefficient of variation of nearest neighbour distances; corr. dim. – correlation dimension (see text); SD – standard deviation; CV(density) – coefficient of variation of estimated density over grid cells. CE, green: statistically not different from 1 (90 % confidence); black: CE>1 (over-dispersed), red: CE<1 (aggregated).
Source: Table created by Peter Bossew.

Station design

Between and even within networks, monitoring stations are designed differently, with different types and models of monitors and detectors utilised. As a consequence, the raw values sent to EURDEP are not entirely comparable, although all measure the same nominal quantity, namely ADER in nSv/h. The following factors control the measured value:

a. Station level

This concerns siting of the monitor. The standard protocol requires that it is located 1 m above even, regionally typical, natural ground without objects such as buildings, trees, waterbodies or roads in its surroundings. Ideally, this "object-free zone" should be a circle with a radius of about 100 m, reflecting the range of "view" of the detector (i.e. the area from which a high percentage of gamma rays originate) although this is often hard to realise in the field. A large proportion of EURDEP stations more or less conform to this protocol, however a number do not as monitors are sometimes mounted on roofs or close to buildings etc. A procedure has been developed to quantify the bias due to deviation of the actual station siting from the ideal (e.g. Zähringer & Sempau, 1996). For terrestrial dose rate, the issue is particulary significant because, for example, a monitor mounted on top of a roof may record the natural radioactivity of building materials rather than from the surrounding ground. Finding close-to-ideal sites is certainly more difficult in densely populated or mountainous regions.

b. Monitor level

The raw ADER value given by the monitor depends on its intrinsic background and on response to the different components of dose rate. Response depends on gamma-ray energy and on radiation type, as it is different for cosmic rays (mainly muons) and gamma rays. Conversion from count rate, which is the initial output into ADER, is made by applying a calibration factor. Depending on the reference gamma-ray energy used in the calibration facility, the same environmental gamma flux may be converted into different ADER values.

c. Detector types

ADR monitors often consist of two detectors, one for low and one for high dose rates. Different detector types are in use, typically Geiger-Müller and proportional counters. Increasingly, spectrometric detectors are being used, the main type currently employing a lathanum-bromide ($LaBr_3$) scintillator. In principle, these monitors allow discrimination between different sources of registered radiation. Different types of monitors are shown in the picture on the right.

d. Quality assurance

For monitoring networks, quality assurance (QA) focuses on monitor and detector level. On network level, design is subject to political conditions, i.e. the objective of the network, but also to economic constraints. There seem to be no procedures of QA for validating the degree to which the planned objective is met.

On monitor and detector level, QA efforts are intense. Detectors are calibrated at certified facilities and characterised in designated experiments and research projects. Important parameters are intrinsic background (self-effect), linearity of energy response and response to cosmic radiation. Literature about the subject is abundant; just to quote a few, we mention the long-term experiment for intercomparison of monitors under real ambient conditions INTERCAL (Bleher et al., 2014). In Europe, the key coordinator for QA is the EURADOS (European Radiation Dosimetry, http://eurados.org/) working group 3, e.g. Wissmann & Sáez-Vergara (2006), Sáez-Vergara et al. (2007), Dombrowski et al. (2009) and Neumaier & Dombrowski (2014). The most recent progress of this EURADOS working group is presented in Vargas (2018).

Data management

Again, data are processed differently and stored at the station by local electronics and transmitted to the network, where other data-processing steps may be performed. Processing steps include subtraction of the intrinsic background and of cosmic radiation, computing averages over several data counting cycles. These can be very short, in the order of seconds, allowing high temporal resolution of a dynamic radiation situation, but inevitably involving high uncertainty in counting. For transmission to EURDEP, 1 hour-averages are computed. For their own purposes, networks may use different aggregation periods. EURDEP performs simple statistics and plots the data. Time series of individual stations can be displayed. Data are being stored permanently.

Dose rate monitors used in European early-warning networks, installed for long-term intercomparisons at the intercalibration site in Schauinsland, Germany.
Source: Picture taken from EURAMET (2017).

Heterogeneity of the EURDEP system

The previous sections showed the high degree of heterogeneity between and even within monitoring networks. Within-network heterogeneity is mostly caused by non-uniform station siting. Between networks, the main differences are due to detector types, calibration procedures and data processing.

Heterogeneity leads to reduced comparability of values. This is of concern if small geographical differences need to be detected, because methodical bias could show difference where there is none or obscure the existing ones. The within-network heterogeneity (mainly due to station siting) may induce a noise component into a geographical picture, which may again obscure true signals.

Therefore, attempts have been made since the early 2000s to harmonise EURDEP, in the sense of identifying and understanding the systematic differences and proposing methods of "top-down" harmonisation. This denotes standardisation procedures that "recalculate" reported values to standardised ones, for example by subtracting intrinsic detector background or the cosmic component, or by labelling stations which should not be compared with standard ones due to their non-standard siting. (This is to be distinguished from "bottom-up" harmonisation, which means having the same measurement conditions and instruments everywhere; evidently, this is not achievable.)

Several studies have been performed on the subject and numerous documents published. One project is AIRDOS (Evaluation of existing standards of measurement of ambient dose rate; and of sampling, sample preparation and measurement for estimating radioactivity levels in air); some documents can be accessed on the EURDEP site (registered users only).

4.3.4 New technical developments

a. Spectrometric detectors

As mentioned, spectrometric detectors are increasingly used for fixed and mobile (see below) monitoring, as new scintillators such as $LaBr_3$, $CeBr_3$, SrI_2 or $Bi_4Ge_3O_{12}$ (BGO) and semiconductors, notably CdZnTe (CZT), are becoming affordable. The appeal of these detectors consists in the possibility of energy resolved in addition to dose rate measurement, which allows gamma radionuclide discrimination, to some extent; but limited only by energy resolution. The recent European research project "MetroERM" has dealt with QA aspects of such detectors being employed in early-warning networks (EURAMET, 2017). To calculate dose rate from gamma spectra, see Dombrowski (2014) and Camp & Vargas (2014).

Apart from higher resolution, the advantages of CZT and new scintillator systems are light weights, which make them interesting for small, unmanned carriers. A drawback of $LaBr_3$ detectors is their internal background, due to the naturally occurring radioisotope ^{138}La (abundance 0.9 %, half-life of 10^{11} years, gamma energies of 789 and 1 436 keV; the former interferes with the 796 and 802 keV peaks of ^{134}Cs, the latter

Influence of site geometry

Figure 4-11 shows the fractions of dose rate originating from discs of different radii. The selected gamma energies are typical for natural terrestrial radionuclides. About 70 to 80 % of gamma dose rate originates from the area within 10 m surrounding the monitor. (In this example, radionuclides are assumed homogeneously distributed on the ground. This is approximately valid for natural radionuclides in most cases.) To capture 90 %, a surrounding of 100 m is necessary. This implies that deviations from the standard site geometry within several 10 m around the monitor can introduce serious bias into the monitor response. Note that the dose rate is also generated by the part of the energy spectrum below the full energy photo peak due to Compton scattering in soil, air, and back-scattering (skyshine). For similar graphs, see Malins et al. (2015).

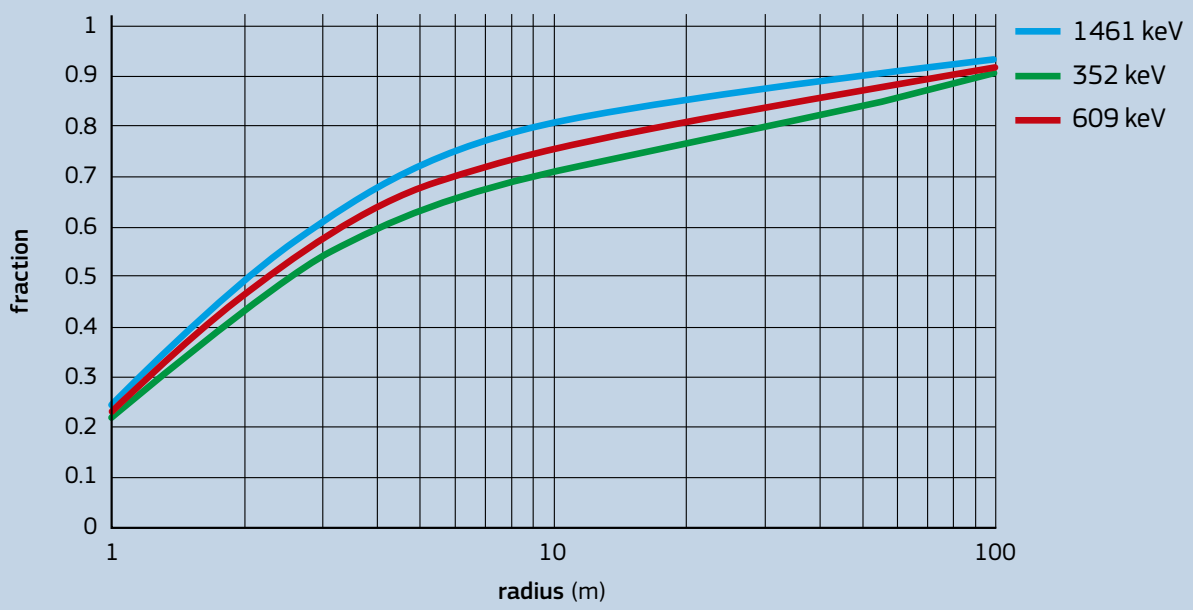

Figure 4-11.
Fraction of the dose rate coming from a disc of given radius around the detector, for three gamma energies characteristic of geogenic radionuclides; source homogeneously distributed in the ground. The detector is located 1 m above ground. From data in Zähringer & Sempau (1997), Table 7.
Source: Bossew et al. (2017).

with ^{40}K, 1 461 keV). Newly available $CeBr_3$ detectors do not have this disadvantage. On the other hand, CZTs, in their current state of development, are comparatively less sensitive. Therefore, they can only be used in situations of relatively high gamma flux, i.e. high levels of contamination.

It appears, up to now, that for airborne gamma-ray spectrometric routine mapping of natural radioactivity, the new systems cannot compete with the 'classical' NaI-detector-based ones. However, Martin et al. (2015) used an unmanned aerial vehicle (UAV; also called a drone) equipped with a CZT detector to map residues around former uranium mines.

b. New monitoring techniques

Fixed monitoring stations, as discussed here, have the advantage that QA is relatively easy, so that these stations yield reliable, reproducible and comparable results (the latter with regard to readings of the same monitor, but in principle also with those of other stations; see discussion above). Their disadvantage lies in their inevitably coarse spatial resolution. Local, 'small' events will likely go unnoticed unless they happen to occur in the immediate vicinity of the station; even if noticed otherwise, their development cannot be followed by fixed stations possibly far away. Moreover, locally high contamination gradients and complex contamination situations in spatial scale below the one of the monitoring network cannot be resolved by these means. As a complement to fixed-station networks, mobile monitoring of different kinds has gained importance, and QA of such systems has been intensively developed for some years. Among the available techniques are car-borne and 'backpack-borne' monitoring (picture below, right) and detectors carried by drones, as these are cheaply available nowadays (picture below, left), or light aircraft (Guastaldi et al., 2013; Alberi et al., 2017).

A very important development is 'crowd-sourced' monitoring, as part of the Citizen Science movement: using quality-assured instruments and protocols, citizens roam the environment and measure dose rate (or other quantities) and transmit the data to a centre where they are further processed. This approach has gained momentum after the Fukushima accident (11 March 2011). The best-known platform seems to be Safecast (https://blog.safecast.org/), which collects dose rate data worldwide and has produced astonishing results. The European research project entitled 'Metrology for mobile detection of ionising radiation following a nuclear or radiological incident' deals with QA aspects of these new techniques, EURAMET (2018).

4.4 Terrestrial dose rate mapping

Natural radiation, composed of cosmic radiation, terrestrial radiation and of radionuclides in air and water sources, varies as a function of latitude and altitude. Terrestrial radiation varies according to the lithology of rocks, genesis and age of rocks and by absorption at the Earth´s surface. Indeed the radioactivity of rocks is widely studied since rocks are the prevailing material for house construction.

Due to physical properties of different types of radiation and their penetration, gamma rays are often detected as a measure of the terrestrial radiation. Gamma-ray fields of regional geological objects or areas can be specified by the dose rate and expressed in nGy/h, or by the rate of photon dose equivalent and expressed in nSv/h.

Dose rate maps provide fundamental knowledge of the natural radiation environment, an initial parameter for the radiation protection. Since rocks are the basic building materials, their radiometric signatures and contents of K, Th and U are studied for their applicability in building industry. Localisation of anomalies of terrestrial gamma dose rate is the fundamental technique for exploring radioactive raw materials, as has been described in numerous publications of the IAEA (1979).

Recently, the potential of terrestrial dose rate maps to serve on the regional scale as predictors of radon risk has been investigated (see Section 5.4).

4.4.1 General overview

As described in Section 4.3, different data sources of ambient dose rate data and measurement techniques are available:

a. Field measurement – dedicated surveys

Extensive radiometric measurements have been performed for geological mapping and surveys of the raw materials. More than fifty percent of the area of the Earth's continents have been covered by airborne and ground gamma-ray surveys, focused predominantly on uranium prospecting (IAEA, 2010). Extensive areas and inaccessible areas have been monitored by airborne surveys, local objects have been investigated by ground measurements. The output of these surveys are maps of natural radioelements in rocks and gamma dose rate of rocks. Since airborne and car-borne gamma-ray surveys produce thousands of registered data, compiled dose rate maps have the capacity to depict irregularities in monitored radiation fields.

Monitoring environmental radiation serves to estimate radiation levels and compare them with national reference standards. Resultant values of these investigations include cosmic radiation, terrestrial radiation and nuclear fallout dose rate. Since the nuclear fallout radiation levels vary over time, the year of measurement is significant.

Field airborne radiometric mapping with high-volume scintillation detectors (30 - 50 l of NaI(Tl)), at a standard height of 60 - 120 m, an airplane speed of 90 - 200 km/h, a field of view up to 400 m and 1 second scans provides numerous radiation data along the flight trajectory. The usual procedure for environmental radiation mapping is filter and aggregate data to a regular grid, corresponding to profile separation, before performing radiometric data contouring. Resultant radiometric dose rate maps (nGy/h) correspond to radiation of large geological bodies.

Ground radiometric measurements, carried out along the profiles or irregular tracks over the area of interest, provides local dose rate data. Fundamental parameters affecting the reliability of the radiometric data are inhomogeneity of the geological basement, geometry of the terrain, change of the background and exposure time of single measurements. Dependence on portable instruments and their calibration results are introduced in dose rate (nGy/h), or in the rate of photon dose equivalent (µSv/h).

Basic references for evaluating airborne gamma-ray spectrometry are Beck et al. (1972), Miller & Shebell (1993), ICRU (1994), IAEA (1991) and IAEA (2003).

b. Monitoring networks

Systematic measurements focused on radioactive raw materials prospecting and localisation of radioactive anomalies are carried out in fixed-line separation, using airborne, car-borne and ground measurements, or rough terrain airborne contouring, while estimates of environmental radiation can also be based on observations at irregularly placed stations in the area of interest. An example of the latter on European scale is the EURDEP system, described in detail in Section 4.3.2.

c. Calculation from geochemical data

Computation of dose rate using known concentration values of natural radioelements K, U and Th in rocks and soils is based on the model of gamma radiation of the homogeneous infinite plane over the Earth´s surface. Constants for conversion of the unit K, U, and Th mass concentration in soil at a height of 1 m above the homogeneous soil surface cited in literature (IAEA, 2003; Will et al., 2003) differ negligibly, depending on selected density of rocks and applied radiation constants. The limiting parameter compiling a dose rate field is the source data. K, U and Th concentrations in surface rocks and soils can be effectively determined by *in situ* gamma-ray spectrometry, where the field of view and corresponding analyses depend on the detector elevation, while geochemical sampling represents local random samples of low mass.

Mapping uncertainty

Apart from the uncertainty of input data from which the maps are made, the mapping procedure itself is also prone to uncertainty. Maps made of sets of methodically different data, even if nominally measuring the same quantity, can therefore look different. This effect is inevitable by physical nature, but it can give rise to misunderstandings and miscommunication, and in consequence to credibility problems.

a. Point samples

'Point samples' of rock or soil have to be interpolated to generate a spatially continuous map. In this context, 'points' mean locations where individual pieces of material have been collected, or small areas from which several pieces have been collected and mixed. Inference to a contiguous map, or 'response surface', involves uncertainty.

Sampling 'points' may not be representative for the quantity which one attempts to assess. If the target is to establish a map of the radiometric background, i.e. the average or 'typical' level over an area, including anomalies that may be small in spatial extension, may distort the picture. Because of their small size, interpolation may yield misleading results, in particular if the samples were originally collected to search for anomalies (e.g. in the framework of mineral exploration), i.e. for a different objective. Such objectives usually result in preferential sampling schemes, which can introduce heavy bias if used for background mapping. The clear separation, conceptually as well as in practice, of background and anomaly is a non-trivial subject, to which large amounts of scientific literature have been devoted.

Interpolation between 'point' samples requires a model of how values at points in a neighbourhood are correlated. The model is usually estimated from available data and is therefore subject to systematic (see above) and random uncertainty, the latter as every estimation procedure. For more details on geostatistical procedures; see Section 2.4.

b. Area samples

Ground-based ADR measurement or *in situ* gamma-ray spectrometry, usually performed at 1 m above ground, generates values that represent a weighted mean over an area whose radius around the location of the instrument extends from several 10s, up

Mobile monitoring. Left: The experimental drone of the German Office for Radiation Protection (BfS), equipped with a CdZnTe detector. Right: 'Walking-borne' and 'Backpack-borne' ground monitoring. Data are automatically geo-referenced and transferred to the base station.
Source: Both pictures from an exercise in the Chernobyl exclusion zone, 2016.

to 100 m, depending on the gamma-ray energies of the source and its distribution in the ground. The weighting function, called point spread function, can be quite complicated; in any case, the result is not a uniform mean over the detector 'horizon' or 'footprint'. The ideal measuring situation is an infinite, even, empty plane, which is evidently not realistic. Deviation from this ideal geometry introduces bias into the result, which is generally difficult to quantify in terms of gamma rays.

c. Remote sensing – airborne gamma-ray spectrometry

In analogy to (b), aerogamma data represent weighted means over rather large areas. Since the carrier (aircraft, helicopter or, more recently, drones) moves, the footprint is elongated along the flight direction.

Footprints overlap along the flight line (and data corresponding to subsequent footprints are therefore strongly correlated), but may be separated perpendicular to the flight line, depending on the distance between flight lines. The resulting anisotropic correlation structure is a challenge for mapping.

The weighting function is even more complex if the surveyed territory is orographically structured and covered by different vegetation or different type of land use. To some degree, correcting for these effects is possible but complicated. Evidently, they are a source of uncertainty that is difficult to quantify.

Also for the (unrealistic) ideal situation, i.e. the infinite even plane, it is not trivial to conclude from footprint-related data to the theoretic value at a point. Deconvolution of areal data is mathematically demanding as a discipline of inverse modelling (similar to generating tomographic pictures) (e.g. Billings et al., 2003; Druker, 2016).

However, if the objective of airborne survey is to detect anomalies and assess the general contamination pattern, these uncertainties matter little. But straightforward comparison with ground-based methods (a) and (b) is problematic.

Examples of national and regional ambient dose rate maps

An overview of some national and regional dose rate surveys is given in Table 4-3. Some of these countries appear to be active in regional surveying, but apparently did not assemble their data into a national database; a notable example is Turkey which has probably covered most of its territory by regional surveys. In many cases, dose rate surveys are not published in international literature, but remain in reports which are often difficult to access. Some of these maps report ambient dose rate, while the others, after subtracting the radiation background, report natural terrestrial radiation (radioactivity of rocks).

Table 4-3.
Some national and regional ambient dose rate surveys in Europe.
Source: Table created by Peter Bossew.

Code	Country	Method	Map?	Reference
AT	Austria	ground measurements	no	Tschirf (1975)
BA	Bosnia and Herzegovina	calculated from samples	no	Pehlivanovic (2016)
BE	Belgium	calculated from samples, TLD, ground measurements	yes	Deworm (1988)
CH	Switzerland	airborne & ground measurements	yes	Rybach (2002)
CZ	Czech Republic	airborne, ground & carborne measurements, geochemical surveys	yes	Manová & Matolín (1995); Matolin (2017)
DE	Germany	ground measurements	yes	Will et al. (1997); Will et al. (2003)
ES	Spain	ground measurements	yes	Quindós-Poncela et al. (2004); García-Talavera et al. (2007, 2013)
IT	Italy / Aeolian Islands	ground measurements	yes	Chiozzi (2001, 2003)
PL	Poland	ground measurements	yes	Strzelecki et. al. (1994)
RS & ME	Serbia, Montenegro	calculated from samples	no	Dragovic (2006)
SK	Slovak Republic	ground measurements	yes	Daniel et al. (1997)
TR	Turkey / Adana	ground measurements	yes	Degerlier (2008)
TR	Turkey / Balikesir	ground measurements	yes	Kapdan (2012)
TR	Turkey / Kayseri	ground measurements	yes	Otsanev (2012)
TR	Turkey / Akkuyu	calculated from samples	no	Özmen (2014)
TR	Turkey / Canakkale	car-borne measurements	yes	Turhan (2012)
TR	Turkey / Kutahia	calculated from samples	no	Sahin (2008)

4.4.2 European Terrestrial Gamma Dose Rate Map

Terrestrial gamma dose rate (TGDR) all over Europe has been estimated from geochemical concentration, according to the UNSCEAR formula, as described in Section 4.3.2.

The input data for the the concentrations of uranium, thorium and potassium in soil have been taken from the European maps (10 km × 10 km grid cells) developed using FOREGS and GEMAS databases. The maps are shown and described in Chapter 3.

The calculation is based on two fundamental assumptions: the secular equilibrium; and homogeneity and standard composition of the soil.

Using 0.7 as a factor to transform the absorbed dose in air to external effective dose to adults (UNSCEAR, 2008), the effective dose due to external exposure from terrestrial radionuclides can be estimated by applying the following formula:

$$D\ (mSv/a) = 0.7\ (Sv/Gy) * TGDR\ (nGy/h) * t * [(1 - OF) + SF * OF] * 10^{-6} \quad (4\text{-}13)$$

where:
TGDR (nGy/h) is the absorbed dose rate estimated in Section 4.3.2;
t is the time of exposure in hours (8 760 h = 1 year);
OF is the occupation factor, 0.8 (UNSCEAR, 2008);
SF is the shielding factors of buildings, 1.4 (UNSCEAR, 2000, Annex B).
As input data for TGDR, the values at 10 km × 10 km grid cells estimated for the European Terrestrial Gamma Dose Map have been used.

The European Annual Terrestrial Gamma Dose Rate Map shows the annual effective dose that a person would receive from terrestrial radiation, if she/he spends all the reference time in a location where the soil has fixed K, Th and U concentrations.

Secular radioactive equilibrium

The secular radioactive equilibrium condition is a very good and useful approximation but not strictly true, in particular for the uranium series, because of the presence of radon gas (^{222}Rn) in the middle of the chain. Actually, its relatively long half-life ($T_{1/2}$=3.82 days) allows radon to escape from the soil matrix, entering into the atmosphere. As a consequence, the most superficial layers of soil are partially depleted by radionuclides belonging to the lower part of the uranium chain, in particular the short-lived radon daughters ^{214}Pb and ^{214}Bi, both very strong gamma emitters. These gamma emitters, once produced in air by radon decay, are distributed along the whole atmospheric column, following more or less the concentration pattern of radon. Therefore a significant reduction of the dose rate is expected, as the gamma irradiation at the receptor point (conventionally, 1 m above the ground) due to the short-lived radon daughters is much weaker than it could have been if there were no radon emanation and all the radionuclides would remain trapped in the soil matrix. Anyway, the contribution of this component is very small (a few nGy/h), although during strong atmospheric inversion conditions it can increase somewhat, since radon and its short-lived daughters remain close to the ground. For that reason, no great errors are expected when assuming a standard value for radon emanation in the calculation, thus neglecting the irradiation coming from the radionuclides suspended in the atmosphere. The fraction of radon escaping from soil is difficult to estimate: values of the order of 20 % – 30 % can be assumed for the most superficial layers, although in some special cases the radon emanation fraction can reach values up to 50 %. Moreover, the value of this parameter is not constant in time, being influenced by rain and changes in the soil humidity. The uncertainty regarding the real value of this fraction is probably one of the most important factors affecting the estimation of the gamma dose rate component due to the uranium series.

More rarely, in some particular soils a substantial break of the radioactive equilibrium conditions can also occur due to complex geochemical processes involving uranium and radium: in these cases the secular equilibrium condition between the upper part of the chain (^{238}U) and the lower part (^{226}Ra) can no longer be assured and therefore TGDR cannot be calculated using the simplified Equations 4-11 or 4-12.

In principle, similar considerations also apply to the thorium series: the presence in the radioactive family of another radon gas isotope, namely ^{220}Rn, can break the secular radioactive equilibrium conditions of the chain. However the much shorter half-life of ^{220}Rn (55.6 seconds) significantly limits the fraction of ^{220}Rn able to escape from the soil matrix. Therefore, for the thorium series, an almost perfect secular equilibrium condition can reasonably be assumed.

Soil homogeneity and composition

The assumption of soil homogeneity, characterised by a unique value for the density and by a unique mass attenuation coefficient $(\mu/\rho)_s$, could seem to be a rather crude approximation of reality. However, it can be shown that the variation of these parameters in the typical accepted ranges only slightly affects the dose rate values. Beck's calculations indicated that the differences in composition and moisture content for most plausible soils result in some variations of the TGDR of about 5 % or less. Moisture content is generally the most important factor influencing the $(\mu/\rho)_s$ values. In Beck's work, the $(\mu/\rho)_s$ values were given for a moisture content ranging from 0 to 25 %. Typical values are usually in the range of 10 % - 20 %. In the calculation, a standard soil composition and moisture content were assumed for all soils: Al_2O_3 (13.5 %), Fe_2O_3 (4.5 %), SiO_2 (67.5 %), CO_2 (4.2 %), H_2O (10 %)

The TGDR, calculated as average values over the grid cells, span a wide range, varying from a minimum of 17 nGy/h (0.14 mSv/a) to a maximum of 189 nGy/h (1.53 mSv/a). These values are of course correlated to the highest uranium, thorium and potassium concentrations. Figure 4-12 shows the distribution of the TGDR values: it looks slightly asymmetrical, with a mean of 62 nGy/h

(0.5 mSv/a) and a median of 59 nGy/h.

The distribution pattern of the calculated terrestrial gamma dose shows a wide area (25 %) of low values (below 50 nGy/h or 0.4 mSv/a) from the Netherlands through Denmark and Northern Germany to Eastern Poland. This area corresponds to the Northern Lowland, which is characterised by a cover of glacial drift deposits related to advances and retreats of the Scandinavian Ice Sheet during the Pleistocene.

Other low-value areas are related to glacial deposits (Northern Finland, Sweden and Norway, and Central Norway) or to fluvial sedimentary basins (Tizsa basin in South-Eastern Hungary, Garonne basin and parts of the Rhone valley in France, the Guadalquivir basin and the Segura and Jucar basins in Spain).

The map shows a pattern of higher values forming a wide arc at the northern margin of the Alps, which seems to be due to high potassium concentrations, which in turn are related to fluvioglacial and fluvial sedimentary supply from the uplifted Alps.

High values occur in the mountain ranges related to the Alpine orogeny (Pyrenees, Alps, Apennine Mountains, Dinaric Alps, Hellenides Carpathians, Balkan Mountains), which incorporate several Cenozoic syn- and postorogenic magmatic bodies along with a metamorphic-overprinted Variscan granitic core.

Areas with the highest values (namely, above 99 nGy/h or 0.71 mSv/a) correspond to the mainly granitic Variscan massifs, relics of the late Paleozoic orogenic belt: North Western Iberian Peninsula; Massif Central, Armorican Massif and Vosges in France; Cornubian Massif in Southwest England; the Ardennes and Rhine Massif, Black Forest, Harz Mountains, Bohemian Massif.

In the Mediterranean areas, high values may be noticed also in Central Italy (Lazio and Campania magmatic areas), Northeast Sardinia (Variscan granitic rocks), Calabria in Southern Italy (a fragment of the Alpine chain), Rhodope mountains in Greece and Bulgaria (Early Cenozoic magmatism).

High values in Eastern Sweden and Southern Finland are connected to the Paleoproterozoic granites, pegmatites and volcano-sedimentary rocks of the Southern Svecofennian Province of the Baltic Shield (Lahtinen, 2012), including uranium mineralisation.

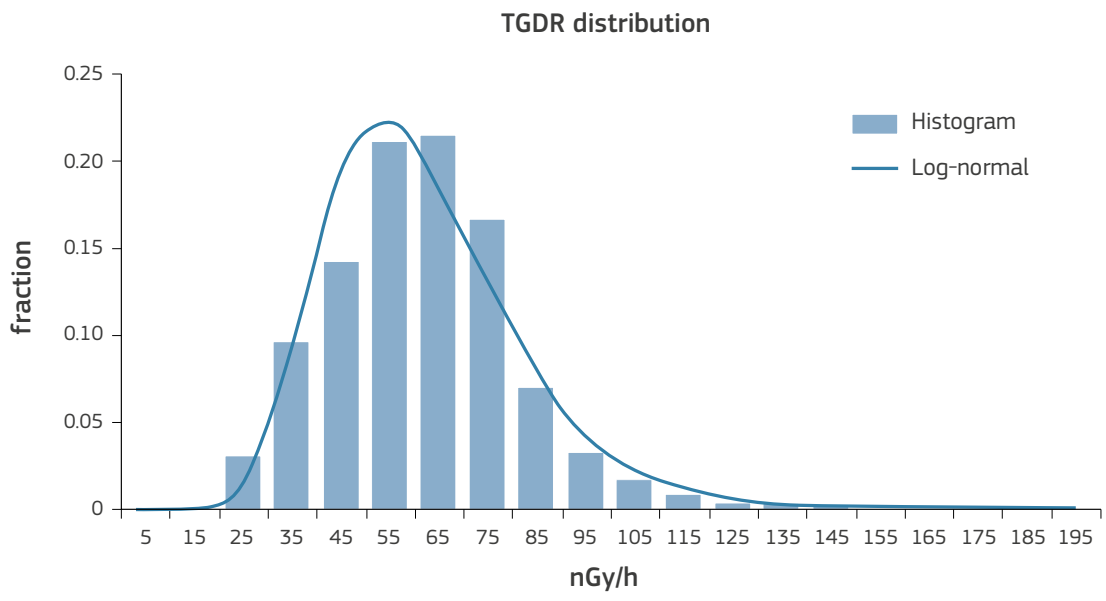

Figure 4-12.
Histogram of TGDR in Europe created with more than 47 000 cells: the distribution is slightly asymmetric and can be fitted with a log-normal function with a mean of 62 nGy/h and a median of 59 nGy/h. Maximum value 189 nGy/h, minimum 19 nGy/h.
Source: EANR, EC-JRC, 2019.

4.4.3 Work in progress: Using EURDEP data to map terrestrial gamma dose rate

Reflecting the geographical variability of external dose rate, the EURDEP network is a natural candidate of a data source for creating ambient dose equivalent rate maps.

In order to identify the contribution from terrestrial natural gamma sources, one has to estimate the contributions of cosmic rays and anthropogenic fallout, and subtract the corresponding dose rates from the total one recorded by the monitor. The different contributions depend on source strengths and on the sensitivity of the probes against these components, as well as on local set-up and mounting of probes. Often, not all factors are exactly known, so that decomposition of the total recorded ADR in order to retrieve the terrestrial natural gamma component is not simple, and problems are multiple:

- ADER is the sum of several components, which need to be disentangled if the objective is mapping of a particular component, notably the terrestrial gamma dose component. This aspect has been discussed in Section 4.2.2.
- Network heterogeneity (see Section 4.3.3):
  a. on network level: this affects precision which depends on station density and geometrical homogeneity;
  b. on station level: this affects comparability of data generated by individual stations.

In spite of large amounts of raw ambient dose rate data available in EURDEP, and many years of efforts to understand in detail and to harmonise the differences between national systems, which is necessary for correct decomposition of the signals, sufficient information is only available for a few countries, namely Austria, Belgium, Croatia, Germany and Hungary. For details, the reader is referred to more extensive discussions in Bossew et al. (2017).

Only for stations from the mentioned countries have the following standardisation steps been performed:

- selection of stations whose siting was deemed to conform sufficiently to the standard;
- calculation and subtraction of site-specific cosmic dose rate (see Section 8);
- subtraction of intrinsic detector background;
- airborne components were deemed of minor relevance;
- artificial fallout, which may locally contribute significantly, was not subtracted because of lack of site-specific information.
- "rain peaks" above and in the next section, were removed.

The value of terrestrial background was defined as the arithmetic mean over long measurement periods (at least 1 year) of the remaining signal. For technical details, the reader is referred to Bossew et al. (2017).

Ordinary kriging has been applied to interpolate the data coming from the above countries. The map, Figure 4-13, shows the gamma dose rate from terrestrial sources (natural plus ^{137}Cs fallout) to which a person would be exposed if she/he spends all the time outdoors. At this stage, ^{137}Cs fallout could not be separated, but in most locations it contributes little (see Bossew et al., 2017). The data do not include the contribution of so-called radon peaks, i.e. radiation of radon progeny deposited on the ground by precipitation. Dose rate generated this way can be quite high in the short-term (up to a few 100 nSv/h), but contributes only in the order of 2 - 5 % to the annual terrestrial gamma dose.

The mapping support is formed by the same 10 km × 10 km cells as for the European Indoor Radon Map (Chapter 5). In this figure, all countries have used nSv/h H*(10) as unit for ambient dose equivalent rate.

As a result, to date, the map of terrestrial ambient dose equivalent rate covers only parts of Europe. In principle, however, the methodology has been established and could be applied to other countries once sufficient technical information becomes available.

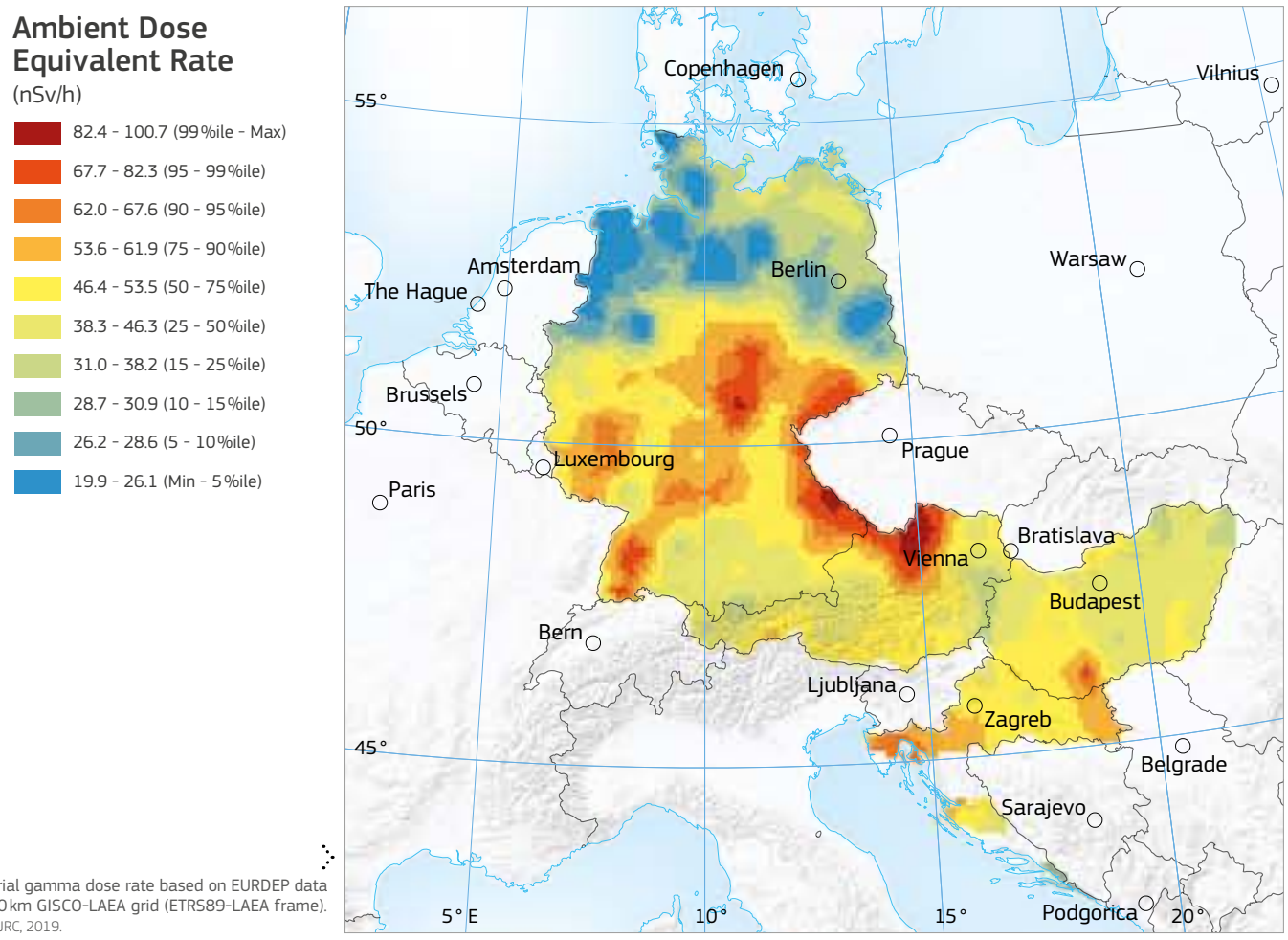

Figure 4-13.
Map of terrestrial gamma dose rate based on EURDEP data on a 10 km × 10 km GISCO-LAEA grid (ETRS89-LAEA frame).
Source: EANR, EC-JRC, 2019.

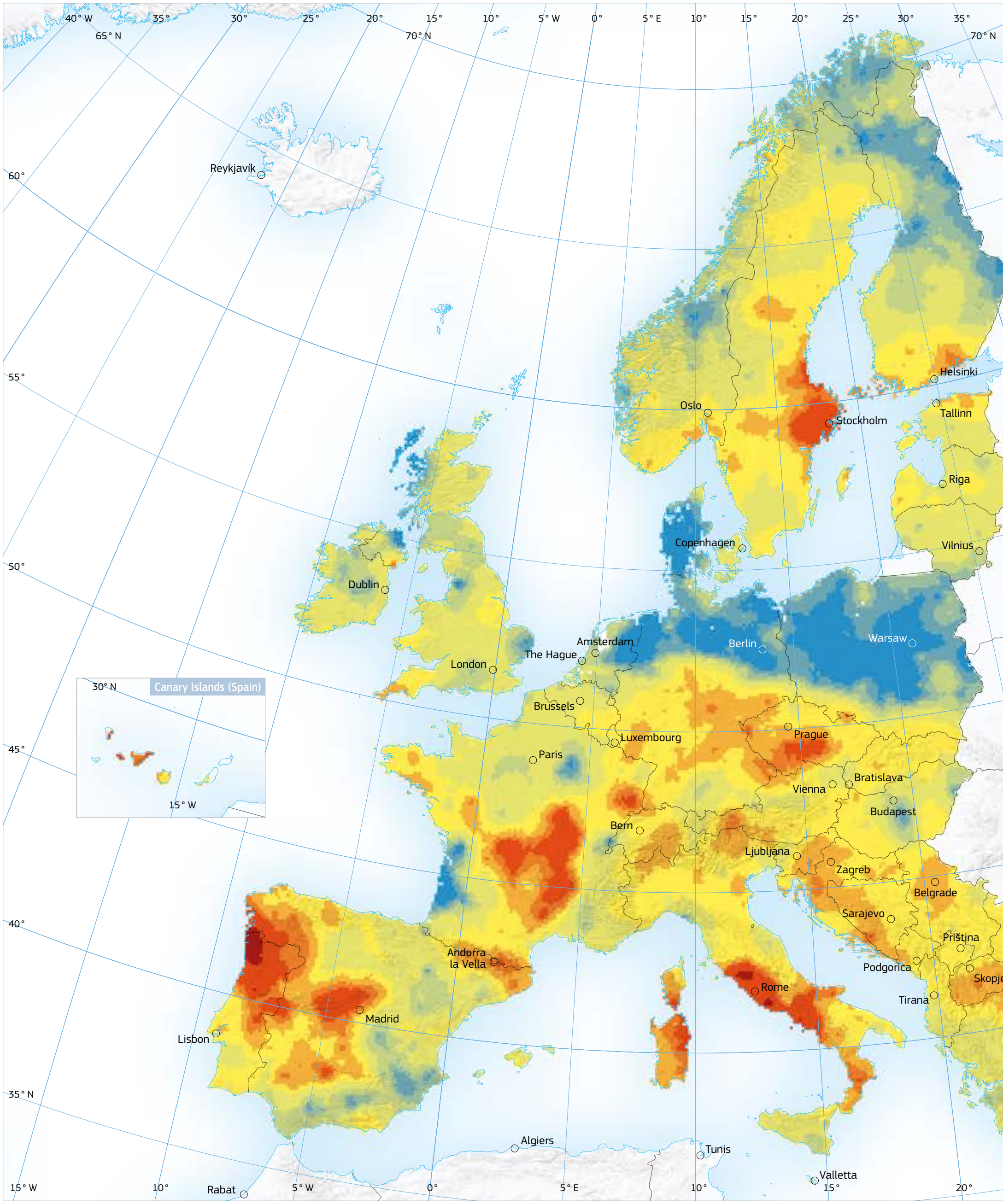
40° W
35°
30°
25°
20°
15°
10°
5° W
0°
5° E
10°
15°
20°
25°
30°
35°
65° N
70° N
70° N
60°
55°
50°
45°
40°
35° N
15° W
10°
5° W
0°
5° E
10°
15°
20°
Reykjavík
Oslo
Stockholm
Helsinki
Tallinn
Riga
Copenhagen
Vilnius
Dublin
London
The Hague
Amsterdam
Berlin
Warsaw
Brussels
Luxembourg
Prague
Paris
Vienna
Bratislava
Budapest
Bern
Ljubljana
Zagreb
Belgrade
Sarajevo
Priština
Podgorica
Skopje
Tirana
Rome
Andorra la Vella
Madrid
Lisbon
Algiers
Tunis
Valletta
Rabat
Canary Islands (Spain)
30° N
15° W

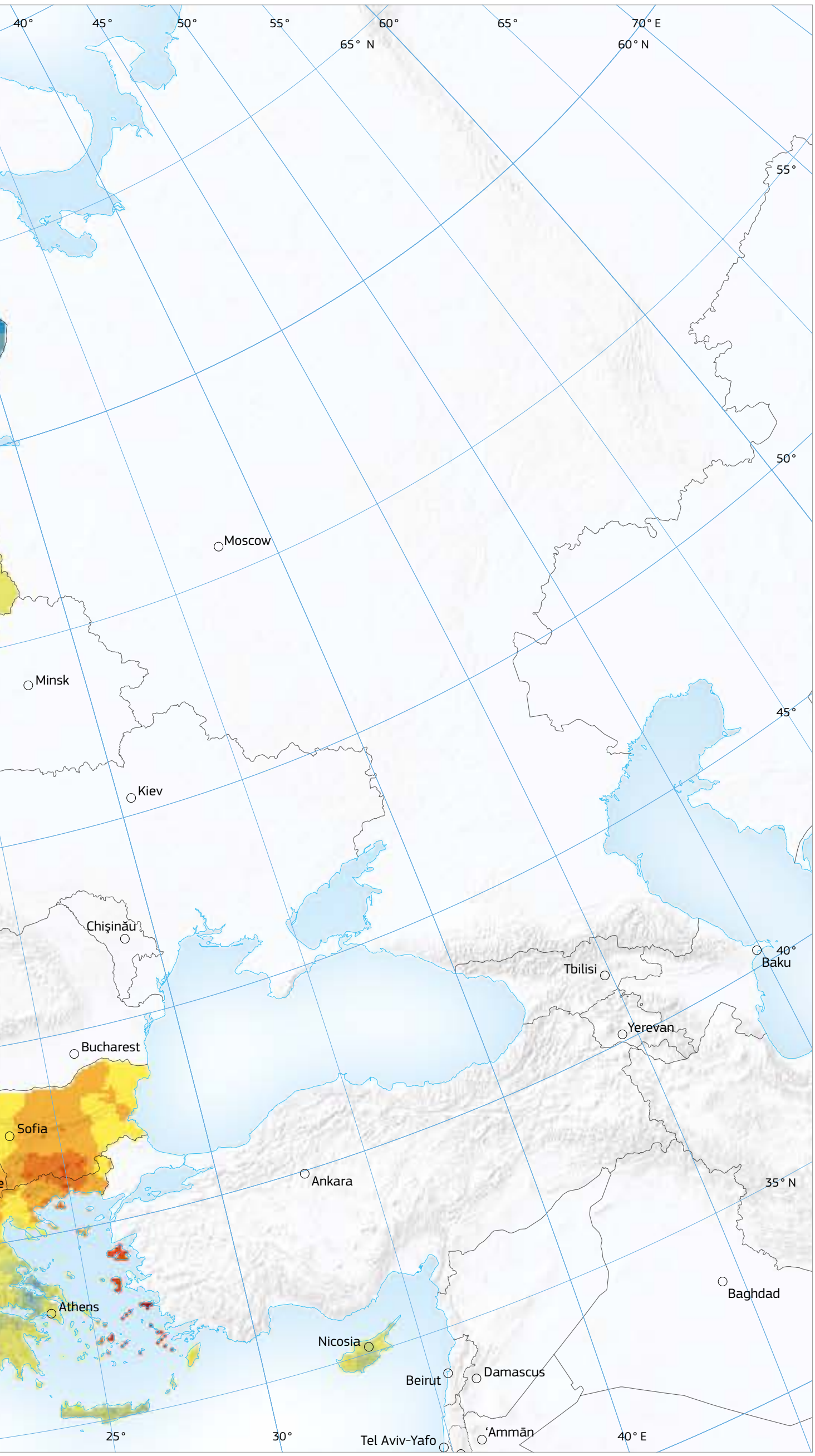

copyright © European Commission, JRC, 2019.

Plate 4: European Terrestrial Gamma Dose Rate Map

(nGy/h)

- 144.3 - 200.0 (99%ile - Max)
- 99.2 - 144.3 (95 - 99%ile)
- 88.5 - 99.2 (90 - 95%ile)
- 75.0 - 88.5 (75 - 90%ile)
- 62.3 - 75.0 (50 - 75%ile)
- 48.8 - 62.3 (25 - 50%ile)
- 41.4 - 48.8 (15 - 25%ile)
- 37.4 - 41.4 (10 - 15%ile)
- 32.0 - 37.4 (5 - 10%ile)
- 32.0 - 37.4 (Min - 5%ile)

Plate 4: European Terrestrial Gamma Dose Rate Map.
The map shows the dose rate, in nGy/h, that a person would receive from terrestrial radiation, if she/he spends all the reference time in a location outdoor in which the soil has fixed U, Th and K concentrations.
Source: EANR, EC-JRC, 2019.

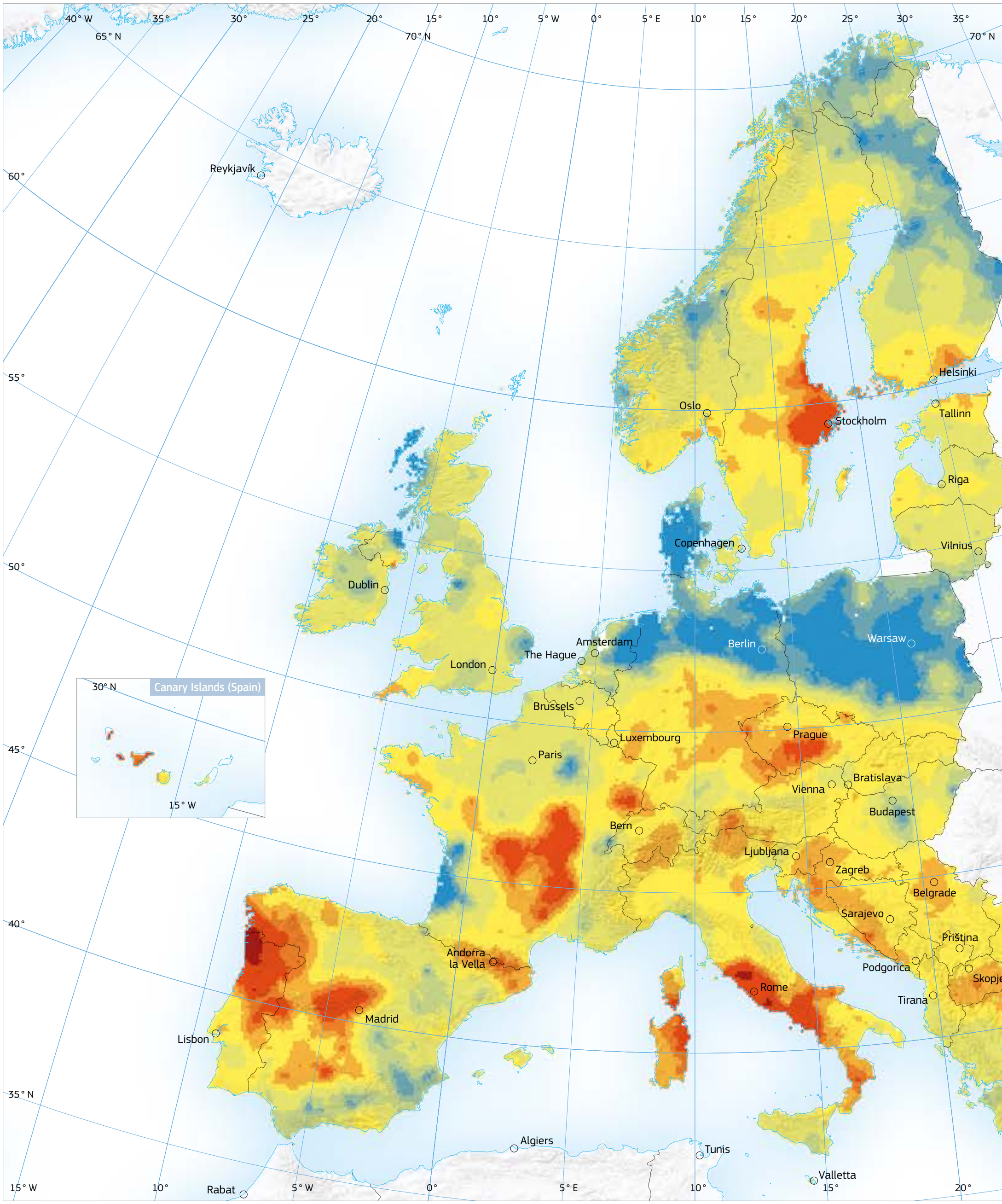
40° W
35°
30°
25°
20°
15°
10°
5° W
0°
5° E
10°
15°
20°
25°
30°
35°
65° N
70° N
70° N
60°
55°
50°
45°
40°
35° N
Reykjavík
Oslo
Helsinki
Stockholm
Tallinn
Riga
Copenhagen
Vilnius
Dublin
Amsterdam
The Hague
Berlin
Warsaw
London
Brussels
Luxembourg
Prague
Paris
Vienna
Bratislava
Budapest
Bern
Ljubljana
Zagreb
Belgrade
Sarajevo
Priština
Podgorica
Skopje
Tirana
Andorra la Vella
Rome
Madrid
Lisbon
Algiers
Tunis
Valletta
Rabat
30° N
Canary Islands (Spain)
15° W
15° W
10°
5° W
0°
5° E
10°
15°
20°

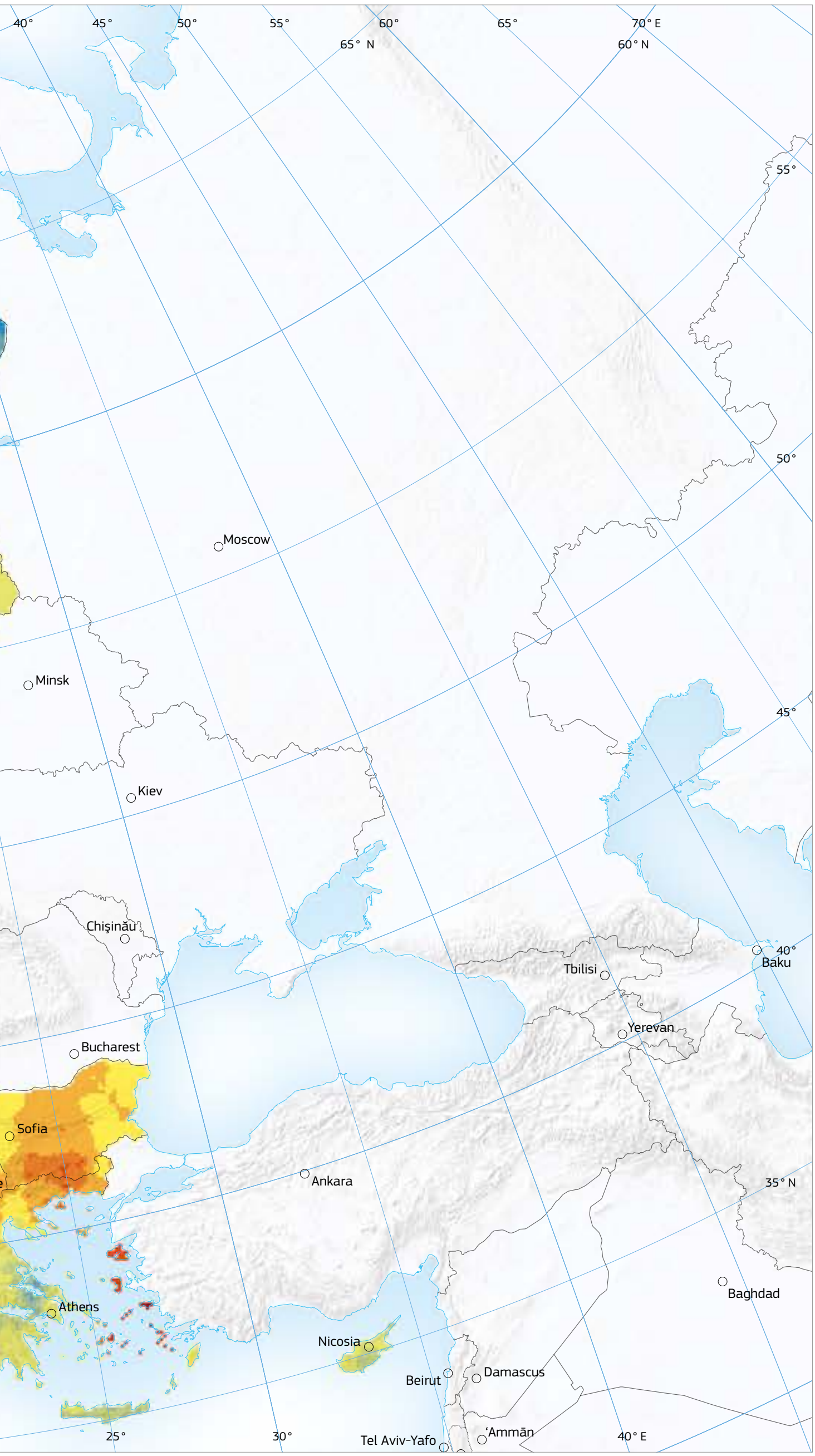

copyright © European Commission, JRC, 2019.

Plate 5: European Annual Terrestrial Gamma Dose Map

(mSv)

- 1.17 - 1.60 (99%ile - Max)
- 0.80 - 1.17 (95 - 99%ile)
- 0.72 - 0.80 (90 - 95%ile)
- 0.61 - 0.72 (75 - 90%ile)
- 0.50 - 0.61 (50 - 75%ile)
- 0.39 - 0.50 (25 - 50%ile)
- 0.33 - 0.39 (15 - 25%ile)
- 0.30 - 0.33 (10 - 15%ile)
- 0.26 - 0.30 (5 - 10%ile)
- 0.14 - 0.26 (Min - 5%ile)

Plate 5: European Annual Terrestrial Gamma Dose Map.
The map shows the annual effective dose in mSv that a person would receive from terrestrial radiation, if she/he spends all the reference time in a location in which the soil has fixed U, Th and K concentrations.
Source: EANR, EC-JRC, 2019.

Case study: Piedmont (Italy), soil and rock samples

While soil databases are convenient for their uniformity over Europe, in some regions concentrations of uranium, thorium and potassium in rocks are made available from gamma spectrometry. Comparison of data in rocks and soils, carried out by relating soil data to the bedrock in regions where both datasets are available, shows that soil data are strongly connected to the bedrock lithology.

Gamma spectrometry of rocks clearly displays a relation between uranium, thorium and potassium concentrations and different classes of lithologies, characterised not only by homogeneity of broadly defined rock types but also by common genetic processes. As an example, in the Alpine regions cenozoic intrusive rocks with upper crustal contamination and late Paleozoic (Variscan) acid igneous rocks show the highest concentrations of natural radionuclides, while mafic and ultramafic rocks and calcareous mesozoic rocks indicate the lowest. Radionuclide concentrations in detrital rocks and sediments reflect their petrographic compositions. In sediments, depositional environments may play a significant role, like high uranium concentration in lacustrine anoxic sediments.

The consistent number of gamma spectrometry measurements (HPGe) of rocks allows consolidating traditional geological units, identified by lithologic, stratigraphic and genetic criteria, into 'radiogeolithological' classes characterised by homogeneity of radionuclide content, yet preserving a defined geological singularity.

Following this approach, a more detailed work was performed in the Piedmont Region, an administrative district in Northwest Italy near the Alpine French border, covering about 25 400 km². Actually, in this area a large set of experimental radioactivity data were available: 154 topsoil samples and 239 rock samples were analysed by means of HPGe gamma spectrometry during several measurement campaigns conducted by ARPA Piemonte (Environmental Protection Agency of Piedmont), allowing for a quantitative determination of the activity concentrations (Bq/kg) of uranium, thorium and potassium.

It was then possible to assign activity concentration values for uranium, thorium and potassium to each of the 26 'radiogeolithological' classes in which Piedmont's geology was classified. The TGDR for Piedmont was then calculated for each cell grid ($TGDR_{cell}$) as a weighted mean of the $TGDR_{RC}$ radiogeolithological values of the RC_j classes present in each cell:

$$TGDR_{cell} = \sum_j w_j \cdot TGDR_{RC_j} \qquad (4\text{-}14)$$

where w_j are proper weights, calculated on an areal basis.

In Figure 4-14 two maps of the TGDR in Piedmont are displayed. The map on the left has been produced following the 'radiogeolithological' approach described in the previous paragraph, using the UNSCEAR formula for the calculation, while on the right the Piedmont TGDR map, simply taken from the European map is shown for comparison. It can easily be seen that in the 'radiogeolithological' map many local peculiarities and details, lost at the European level, appear: some high background areas (TGDR > 120 nGy/h), in particular located along the Alpine ridge, can easily be identified.

Similar, more detailed maps could also be produced for any other European region, provided that a convenient radiogeolithogical database is available.

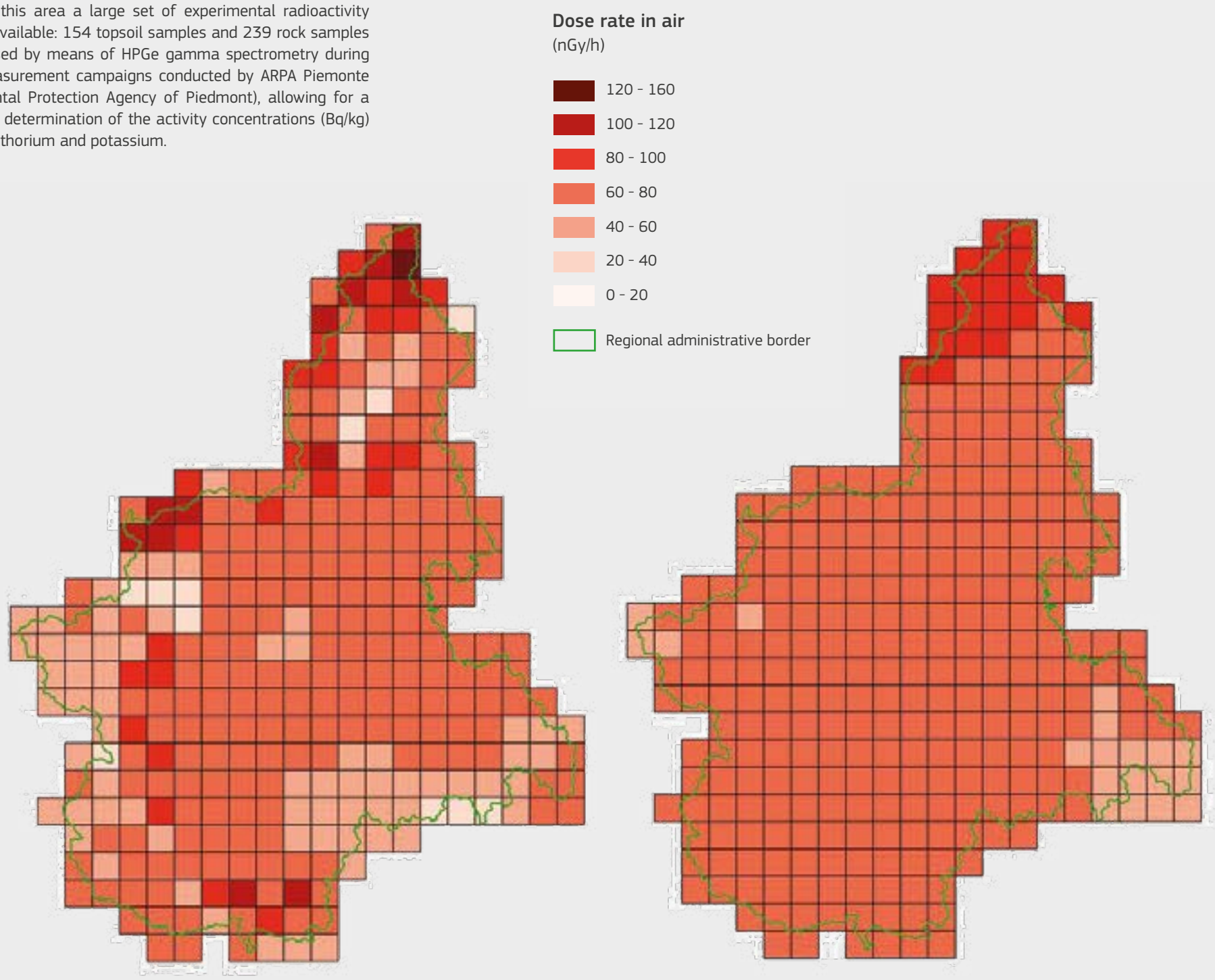

Figure 4-14.
On the left, the 'radiogeolithological' Piedmont's map compared with the 'UNSCEAR map' (extracted from the European Terrestrial Gamma Dose Rate Map): it provides more detailed local radiological information that is lost at greater scale.
Source: Cinelli et al., 2018.